# The evolution of unpolarized singlet structure functions at small $x$

Johannes Blümlein

*DESY-Zeuthen, Platanenallee 6, D-15735 Zeuthen, Germany*

Andreas Vogt

*Institut für Theoretische Physik, Universität Würzburg, Am Hubland, D-97074 Würzburg, Germany*

A systematic study is performed of the impact of the various resummed small-$x$ contributions to the anomalous dimensions and coefficient functions on the evolution of unpolarized structure functions in deep-inelastic scattering. The proton structure functions $F_2^p$ and $F_L^p$ as well as the photon structure function $F_2^\gamma$ are considered together with the corresponding parton densities. The general analytic solution of the evolution equations in Mellin-$N$ space is derived, and different approximate solutions are compared. Potential effects of less singular small-$x$ terms in the anomalous dimension and coefficient functions are discussed. [S0556-2821(98)02413-8]

## I. INTRODUCTION

One of the central questions in the theory of deep-inelastic scattering (DIS) structure functions is that of their behavior at small values of the Bjorken $x$. The experiments at the DESY $ep$ collider HERA [1] have performed detailed measurements of the structure function $F_2(x,Q^2)$ down to values of $x \simeq 10^{-5}$ and have presented first results on $F_L(x,Q^2)$ in the range $x \gtrsim 10^{-4}$ [2]. $F_2$ rises even at small values of $Q^2 \sim 2$ GeV$^2$ approximately as $x^{-0.2}$. At low scales $Q^2$ the behavior of structure functions cannot be dealt with by means of perturbative QCD due to the size of the strong coupling constant $\alpha_s(Q^2)$. For large virtualities, on the other hand, a perturbative description of the scaling violations is possible if a factorization can be achieved between the non-perturbative input distributions and the evolution kernels which can be calculated perturbatively.

Throughout the present paper we will consider deep-inelastic scattering in the range where it is dominated by the light-cone singularities in the Bjorken limit, $Q^2, s \to \infty$, $x = Q^2/(sy) = \text{const}$, with $Q^2$ the 4-momentum transfer squared, $s$ the center-of-mass energy, $y = 2P \cdot q/s$. The ultraviolet singularities of the operators emerging in the light-cone expansion [3] are associated with renormalization group equations (RGEs) which describe the evolution of the structure functions. Under these conditions the evolution kernels are given by the anomalous dimensions of the light-cone operators. For the leading-twist contributions considered in the following, the expectation values of the operators are related to the parton distribution functions. This picture holds, in principle, down to the region of small values of $x$. The anomalous dimensions and coefficient functions, however, may receive large low-$x$ contributions of the type [4]

$$\alpha_s^l \left( \frac{\alpha_s}{N-1} \right)^k \leftrightarrow \frac{1}{x} \alpha_s^{l+k} \frac{\ln^{k-1}(1/x)}{(k-1)!},$$

where $N$ denotes the index of the Mellin-transformation

$$\mathcal{M}[f(x)](N) = \int_0^1 dx\, x^N f(x).$$

The $x$-range in which this representation is applicable can only be determined by explicit calculations [5] and depends on both the behavior of the partonic input densities at a starting scale $Q_0^2$ and on the structure of the anomalous dimensions and coefficient functions. Note that the present picture does not necessarily yield a description of the structure functions as well in the Regge limit $s \to \infty, Q^2 = \text{const}$, since both limits lead in general to different results. This can be seen [6] performing these limits in the Jost-Lehmann-Dyson representation [7] of the structure functions.

In the Bjorken limit the ultraviolet and collinear divergences emerging in the calculation of the higher-order corrections can be dealt with applying the corresponding RGE-operators, which imply the evolution of the parton densities and the running of the strong coupling constant. The resummed small-$x$ corrections in leading [4] and next-to-leading order [8–10] can thus be accounted for in a natural way. Since the impact of the resulting all-order anomalous dimensions on the behavior of the DIS structure functions at small $x$ does as well depend on the non-perturbative input parton densities at an initial scale $Q_0^2$, the perturbative resummation effects can only be studied via the evolution over some range in $Q^2$. This evolution probes also the anomalous dimensions and coefficient functions at medium and large values of $x$ due to the Mellin convolution between the evolution kernels and the parton densities; cf. Ref. [11]. Hence the small-$x$ dominance of the leading terms over less singular contributions as $x \to 0$ in the anomalous dimensions and coefficient functions does not necessarily imply the same effect for the observables, such as the structure functions.

In the present paper a systematic study is performed on the impact of the different resummed small-$x$ contributions to the anomalous dimensions and coefficient functions on the evolution of the singlet contributions to the nucleon structure functions $F_2(x,Q^2)$ and $F_L(x,Q^2)$. A brief summary of some of our numerical results on the effects of the resummed gluon anomalous dimension on the nucleon structure functions has already appeared in [12]. We extend the analysis to the photon structure function $F_2^\gamma(x,Q^2)$, for which we derive corresponding results in the DIS scheme.

The paper is organized as follows. The general framework for the evolution of parton densities of the nucleon and the photon is recalled in Sec. II. In Sec. III the presently known small-$x$ resummed anomalous dimensions and coefficient functions [4,8–10] are summarized and the numerical coefficients for their expansions in $\alpha_s$ are compiled for the subsequent analysis. The issue of less singular terms is discussed in Sec. IV guided by the known 2-loop results. In Sec. V different methods are derived for the solution of the evolution equations in the presence of all-order resummations for the small-$x$ contributions. The numerical implications of the small-$x$ resummations on the evolution of the parton densities and the structure functions $F_2^p$, $F_L^p$ and $F_2^\gamma$ are worked out in detail in Sec. VI for typical sets of initial distribution. Section VII contains our conclusions.

## II. THE EVOLUTION EQUATIONS

The twist-2 contributions to the structure functions in inclusive deep-inelastic scattering can be described in terms of the QCD-improved parton model. Their scaling violations are governed by renormalization group equations which can be formulated to all orders in the strong coupling constant. In this section we briefly recall this general framework, which allows for a consistent introduction of the small-$x$ resummations into the structure function evolution, and its specific application to hadronic and photonic parton distributions.

### A. The renormalization group equations

Among the singularities emerging in the calculation of QCD radiative corrections, only the ultraviolet divergences and the initial-state mass singularities require a special treatment in inclusive deep-inelastic scattering.[1] The former are eliminated by the renormalization of the strong coupling constant. The remaining mass singularities, originating in collinear emissions of massless partons off massless partons, are removed by mass factorization; i.e., these contributions are absorbed into the bare parton densities. For this procedure the structure functions $F_i(x,Q^2)$ are first written as

$$F_i(x,Q^2) = \hat{F}_{i,k}\left(x,\alpha_s(R^2),\frac{Q^2}{\mu^2},\frac{R^2}{\mu^2},\varepsilon\right) \otimes \hat{f}_k(x). \quad (2.1)$$

Here $\alpha_s(R^2)$ denotes the strong coupling constant, renormalized at the scale $R$ in some renormalization scheme. $\mu$ is an arbitrary mass scale. $\hat{f}_k$ represents the bare momentum distribution of the parton species $k$, and $\otimes$ stands for the Mellin convolution in the first variable:

___
[1] The infrared divergences cancel between the virtual and Bremsstrahlung contributions according to the Bloch-Nordsieck theorem [13]. The final-state mass singularities vanish due to the Kinoshita-Lee-Nauenberg theorem [14], as all degenerate final states are summed over.

$$A(x,\mu_a^2) \otimes B(x,\mu_b^2)$$
$$= \int_0^1 dx_1 \int_0^1 dx_2\, \delta(x-x_1 x_2) A(x_1,\mu_a^2) B(x_2,\mu_b^2). \quad (2.2)$$

Finally $\varepsilon$ marks the initial-state mass singularities entering the bare partonic structure functions $\hat{F}_{i,k}$. These functions are then separated into the coefficients functions $C_{i,j}$ and the transition functions $\Gamma_{jk}$, which contain the $1/\varepsilon$ pole terms, according to

$$\hat{F}_{i,k}\left(x,\alpha_s(R^2),\frac{Q^2}{\mu^2},\frac{R^2}{\mu^2},\varepsilon\right)$$
$$= C_{i,j}\left(x,\alpha_s(R^2),\frac{Q^2}{M^2},\frac{R^2}{M^2}\right) \otimes \Gamma_{jk}\left(x,\alpha_s(R^2),\frac{M^2}{\mu^2},\frac{M^2}{R^2},\varepsilon\right). \quad (2.3)$$

The additional parameter $M$ is the factorization scale. This separation is not unique beyond the leading order (LO) of the perturbative expansion; hence $\Gamma_{kj}$ and $C_{i,k}$ are also factorization scheme dependent. Combining Eqs. (2.1) and (2.3), the structure functions $F_i(x,Q^2)$ finally read

$$F_i(x,Q^2)$$
$$= C_{i,j}\left(x,\alpha_s(R^2),\frac{Q^2}{M^2},\frac{R^2}{M^2}\right) \otimes f_j\left(x,\alpha_s(R^2),\frac{M^2}{\mu^2},\frac{M^2}{R^2}\right) \quad (2.4)$$

in terms of the renormalized parton densities $f_j$ given by

$$f_j\left(x,\alpha_s(R^2),\frac{M^2}{\mu^2},\frac{M^2}{R^2}\right)$$
$$= \Gamma_{jk}\left(x,\alpha_s(R^2),\frac{M^2}{\mu^2},\frac{M^2}{R^2},\varepsilon\right) \otimes \hat{f}_k(x). \quad (2.5)$$

Two arbitrary scales, $R$ and $M$, are thus introduced by the renormalization and mass factorization procedures. These scales are not physical. Hence observables, such as the structure functions $F_i(x,Q^2)$ in Eq. (2.4), do not depend on them. Since the ultraviolet and mass singularities are not related, the conditions

$$R^2 \frac{d}{dR^2} F_i(x,Q^2) = 0, \quad (2.6)$$

$$M^2 \frac{d}{dM^2} F_i(x,Q^2) = 0 \quad (2.7)$$

hold separately and imply two independent renormalization group equations. The first of these equations leads to the scale dependence of the running coupling constant:

$$\frac{da_s}{d\ln R^2} = \beta(a_s) \equiv -\sum_{l=0}^{\infty} a_s^{l+2} \beta_l, \qquad (2.8)$$

where the abbreviation $a_s = \alpha_s(R^2)/(4\pi)$ has been introduced for convenience. At next-to-leading order (NLO) only the first two scheme independent terms [15,16] of $\beta(a_s)$ are kept,

$$\beta_0 = \frac{11}{3} C_A - \frac{4}{3} T_F,$$

$$\beta_1 = \frac{34}{3} C_A^2 - \frac{20}{3} C_A T_F - 4 C_F T_F. \qquad (2.9)$$

The QCD color factors are $C_F = (N_c^2 - 1)/(2N_c) \equiv 4/3$, $C_A = N_c \equiv 3$, $T_R = 1/2$, and $T_F = N_f T_R$, with $N_f$ denoting the number of light quark flavors. To this approximation, the solution of Eq. (2.8) can be expressed in terms of the QCD scale parameter $\Lambda_{N_f}$ by

$$\frac{1}{\beta_0 a_s} - \frac{\beta_1}{\beta_0^2} \ln\left(\frac{1}{\beta_0 a_s} + \frac{\beta_1}{\beta_0^2}\right) = \ln\left(\frac{R^2}{\Lambda_{N_f}^2}\right). \qquad (2.10)$$

It turns out, moreover, that higher coefficients $\beta_{l \geqslant 2}$ — $\beta_2$ and $\beta_3$ have been calculated in the modified minimal subtraction ($\overline{\text{MS}}$) scheme [17,18]—are not required in connection with the presently available small-$x$ resummations; see Sec. V C. We will therefore employ the relation (2.10) for all our numerical calculations in Sec. VI.

### B. Hadronic and photonic parton densities

The second renormalization group equation (2.7) leads to the scale evolution of the renormalized parton densities $f_j(x, M^2)$. Considering first the hadronic case, the relevant parton species are the quarks and antiquarks, $q_j$ and $\bar{q}_j$, and the gluon $g$. It is convenient to introduce flavor non-singlet combinations of the quark densities,

$$q_j^{\pm} = q_j \pm \bar{q}_j - \frac{1}{N_f} \sum_{r=1}^{N_f} [q_r \pm \bar{q}_r], \qquad (2.11)$$

$$q^{\text{val}} = \sum_{r=1}^{N_f} [q_r - \bar{q}_r], \qquad (2.12)$$

and the singlet quark/gluon vector

$$\mathbf{q} = \begin{pmatrix} \Sigma \\ g \end{pmatrix}, \quad \Sigma \equiv \sum_{r=1}^{N_f} [q_r + \bar{q}_r]. \qquad (2.13)$$

This decomposition decouples the $2N_f + 1$ evolution equations as far as possible by symmetry considerations alone. For simplicity, we will choose the renormalization and fac-

torization scales as $R^2 = M^2 = Q^2$ from now on.[2] The hadronic evolution equations can then be written as

$$\frac{\partial q_j^{\pm}(x, Q^2)}{\partial \ln Q^2} = P^{\pm}(x, a_s) \otimes q_j^{\pm}(x, Q^2),$$

$$\frac{\partial \mathbf{q}(x, Q^2)}{\partial \ln Q^2} = \mathbf{P}(x, a_s) \otimes \mathbf{q}(x, Q^2). \qquad (2.14)$$

The evolution of $q^{\text{val}}$ is identical to that of $q^-$ up to NLO. As our present analysis is confined to that approximation in the non-singlet sector,[3] the corresponding equation has been suppressed in Eqs. (2.14). In general, the splitting functions $P^{\pm}$, $\mathbf{P}$ are given by the infinite series

$$P^{\pm}(x, a_s) = \sum_{l=0}^{\infty} a_s^{l+1} P_l^{\pm}(x),$$

$$\mathbf{P}(x, a_s) \equiv \begin{pmatrix} P_{qq}(x, a_s) & P_{qg}(x, a_s) \\ P_{gq}(x, a_s) & P_{gg}(x, a_s) \end{pmatrix} = \sum_{l=0}^{\infty} a_s^{l+1} \mathbf{P}_l(x). \qquad (2.15)$$

The expansion coefficients $P_l^-(x)$ and $\mathbf{P}_l^{\text{unpol}}(x)$ are, in sensible factorization schemes, subject to the sum rules

$$\int_0^1 dx \; P_l^-(x) = 0, \qquad (2.16)$$

$$\int_0^1 dx\, x \sum_j \; P_{jk,l}^{\text{unpol}}(x) = 0, \qquad (2.17)$$

which are due to fermion number and energy-momentum conservation, respectively. By now all unpolarized and polarized entries in Eqs. (2.15) are completely known at NLO, $l = 1$. The full expressions for their $x$-dependences can be found in Refs. [24–28]. Beyond this order a series of integer Mellin moments of $P_2^+(x)$ and $\mathbf{P}_2(x)$ has been calculated so far [29].

We now turn to the parton densities of the real photon. The photon is a genuine elementary particle, unlike the hadrons. Hence it can directly take part in hard scattering processes, in addition to its quark and gluon distributions arising from quantum fluctuations, $q^{\gamma}(x, Q^2)$ and $g^{\gamma}(x, Q^2)$. Denoting the corresponding photon distribution in the photon by $\Gamma^{\gamma}(x, Q^2)$, the evolution equations for these parton densities are generally given by [30]

---

[2]See Refs. [19,20] for studies of the uncertainties in NLO analyses due to the variation of $R$ and $M$.

[3]The generating relations for the resummation of the anomalous dimensions [21] of the $\pm$ non-singlet combinations were derived in Ref. [22]. Here the leading small-$x$ terms are of $O[(\alpha_s \ln^2 x)^n]$. The effect of these terms has turned out to be on the 1% level down to very small values of $x$ [21,23]. As the non-singlet contributions are furthermore suppressed compared to the singlet ones at low $x$, these resummations are not included in the present treatment.

$$\frac{\partial q_i^\gamma}{\partial \ln Q^2} = a_{em} \bar{P}_{q_i \gamma} \otimes \Gamma^\gamma + a_s \left\{ 2 \sum_{k=1}^{N_f} \bar{P}_{q_i q_k} \otimes q_k^\gamma + \bar{P}_{q_i g} \otimes g^\gamma \right\},$$

$$\frac{\partial g^\gamma}{\partial \ln Q^2} = a_{em} \bar{P}_{g\gamma} \otimes \Gamma^\gamma + a_s \left\{ 2 \sum_{k=1}^{N_f} \bar{P}_{g q_k} \otimes q_k^\gamma + \bar{P}_{gg} \otimes g^\gamma \right\},$$

$$\frac{\partial \Gamma^\gamma}{\partial \ln Q^2} = a_{em} \bar{P}_{\gamma\gamma} \otimes \Gamma^\gamma + a_{em} \left\{ 2 \sum_{k=1}^{N_f} \bar{P}_{\gamma q_k} \otimes q_k^\gamma + \bar{P}_{\gamma g} \otimes g^\gamma \right\}. \tag{2.18}$$

Here $a_{em} \equiv \alpha/(4\pi)$ with the electromagnetic coupling constant $\alpha \simeq 1/137$. The antiquark distributions do not occur separately in Eqs. (2.18), as $\bar{q}_i^\gamma(x,Q^2) = q_i^\gamma(x,Q^2)$ due to charge conjugation invariance. The generalized splitting functions read

$$\bar{P}_{ij}(x,a_{em},a_s) = \sum_{l,m=0} a_{em}^m a_s^l \bar{P}_{ij}^{(m,l)}(x), \tag{2.19}$$

with $\bar{P}_{q_i q_k}$ being the average of the quark-quark and antiquark-quark splitting functions.

Usually calculations involving the photon's parton structure are restricted to the first order in $\alpha \ll 1$. In this approximation all $m \neq 0$ terms in Eq. (2.19) can be neglected, since $q_i^\gamma$ and $g^\gamma$ are already of order $\alpha$. This reduces the functions $\bar{P}_{ij}$ to the usual QCD quantities $P_{ij}(x,\alpha_s)$, and $P_{\gamma q_i}$ and $P_{\gamma g}$ drop out completely. Moreover, one has $P_{\gamma\gamma} \propto \delta(1-x)$ to all orders in $\alpha_s$, as real photon radiation from photons starts at order $\alpha^2$ only. Thus the last line of Eq. (2.18) can be integrated immediately, at LO ($l=0$), for example, resulting in

$$\Gamma_{LO}^\gamma(x,Q^2) = \delta(1-x) \left[ 1 - 4a_s \left( \sum_{k=1}^{N_f} e_{q_k}^2 \ln \frac{Q^2}{Q_0^2} + \text{const} \right) \right], \tag{2.20}$$

where $e_{q_k}$ represents the quark charges, and $Q_0^2$ is some reference scale for the evolution. Only the $O(1)$ part of $\Gamma^\gamma$ affects the quark and gluon densities at order $\alpha$, as well as any observable involving hadronic final states like $F_2^\gamma$. Therefore, after decomposing into the singlet and non-singlet parts as before, one obtains the inhomogeneous evolution equations

$$\frac{\partial q_j^{\gamma+}(x,Q^2)}{\partial \ln Q^2} = k_j^+(x,a_s) + P^+(x,a_s) \otimes q_j^{\gamma+}(x,Q^2),$$

$$\frac{\partial \boldsymbol{q}^\gamma(x,Q^2)}{\partial \ln Q^2} = \boldsymbol{k}(x,a_s) + \boldsymbol{P}(x,a_s) \otimes \boldsymbol{q}^\gamma(x,Q^2). \tag{2.21}$$

Here we have switched to the conventional notation for the photon-parton splitting functions

$$k^+(x,\alpha_s) = \sum_{l=0}^\infty a_{em} a_s^l k_l^+(x),$$

$$\boldsymbol{k}(x,a_s) \equiv \begin{pmatrix} P_{q\gamma}(x,a_s) \\ P_{g\gamma}(x,a_s) \end{pmatrix} = \sum_{l=0}^\infty a_{em} a_s^l \boldsymbol{k}_l(x). \tag{2.22}$$

These splitting functions are presently also known up to NLO ($l=1$); see Refs. [30–32].

### C. Factorization scheme transformations

As stated above, the separation between the coefficient functions and the splitting functions is not unique beyond the leading order. In this subsection, we derive the general factorization-scheme invariants and specify the schemes for our subsequent numerical calculation. We study the photonic case, as the hadronic problem forms a subset hereof. In order to specify the transformation matrices, it is convenient to introduce a fictitious second, ''gluonic'' structure function, where the gluon density enters at order $a_s^0$, but the quarks only at order $a_s^1$, opposite to the situation with the real electromagnetic current; see Refs. [33,34]. This can be formally achieved, e.g., by adding a color-neutral scalar-gluon coupling $\phi F^{\mu\nu} F_{\mu\nu}$ to the QCD Lagrangian. The general singlet structure function $F_2$ then reads

$$\boldsymbol{F}_2 = \begin{pmatrix} F_{2,\gamma} \\ F_{2,\phi} \end{pmatrix} = \langle e^2 \rangle [ \boldsymbol{C}(x,a_s) \otimes \boldsymbol{q}(x,a_s) + \boldsymbol{C}_\gamma(x,a_s) ] \tag{2.23}$$

with

$$\boldsymbol{C}(x,a_s) = \begin{pmatrix} C_{\gamma q}(x,a_s) & C_{\gamma g}(x,a_s) \\ C_{\phi q}(x,a_s) & C_{\phi g}(x,a_s) \end{pmatrix} = \sum_{l=0}^\infty a_s^l \boldsymbol{C}_l(x),$$

$$\boldsymbol{C}_\gamma(x,a_s) = \begin{pmatrix} C_{\gamma\gamma}(x,a_s) \\ C_{\phi\gamma}(x,a_s) \end{pmatrix} = \sum_{l=0}^\infty a_{em} a_s^l \boldsymbol{C}_{\gamma,l+1}(x). \tag{2.24}$$

Here $\langle e^2 \rangle$ is the average squared charge of the light quark flavors, and $\boldsymbol{C}_0$ the unit matrix times $\delta(1-x)$. Using the scale dependence (2.21) of the partons and Eq. (2.8) for the running coupling, the scaling violations of $F_2$ can be written as

$$\frac{d\boldsymbol{F}_2}{d\ln Q^2} = \langle e^2 \rangle [ \boldsymbol{C} \otimes \boldsymbol{k} + \beta \boldsymbol{C}_\gamma'$$

$$- (\boldsymbol{C} \otimes \boldsymbol{P} \otimes \boldsymbol{C}^{-1} + \beta \boldsymbol{C}' \otimes \boldsymbol{C}^{-1}) \otimes \boldsymbol{C}_\gamma ]$$

$$+ (\boldsymbol{C} \otimes \boldsymbol{P} \otimes \boldsymbol{C}^{-1} + \beta \boldsymbol{C}' \otimes \boldsymbol{C}^{-1}) \otimes \boldsymbol{F}_2, \tag{2.25}$$

where the prime denotes the derivative with respect to $a_s$. Both $d\boldsymbol{F}_2/d\ln Q^2$ and $\boldsymbol{F}_2$ represent observables; hence the following combinations of splitting functions and coefficient functions are factorization scheme invariant:

$$I_{\text{hom}} = C \otimes P \otimes C^{-1} + \beta C' \otimes C^{-1}, \qquad (2.26)$$

$$I_{\text{inhom}} = C \otimes k + \beta C_\gamma' - I_{\text{hom}} \otimes C_\gamma. \qquad (2.27)$$

Putting back the perturbative expansions of all quantities involved, these invariants are given order-by-order in $a_s$ [33,34,32] by

$$I_{\text{hom}} = a_s P_0 + a_s^2 \{P_1 + C_1 \otimes P_0 - P_0 \otimes C_1 - \beta_0 C_1\} + \cdots, \qquad (2.28)$$

$$I_{\text{inhom}} = a_{\text{em}} k_0 + a_{\text{em}} a_s \{k_1 + C_1 k_0 - P_0 C_{\gamma,1}\} + \cdots. \qquad (2.29)$$

The generalization to higher orders is straightforward if cumbersome. From these relations the changes $\Delta P$ and $\Delta k$ of the splitting functions induced by a modification of the coefficients $\Delta C$ and $\Delta C_\gamma$ can be easily determined. Recall, however, that a particular choice for the physical upper-row (electromagnetic) quantities $C_{\gamma q}$, $C_{\gamma g}$ and $C_{\gamma\gamma}$ does not fully fix the transformation, as is well-known for the hadronic DIS factorization scheme [35]. In fact, we will use the DIS scheme for our subsequent numerical calculations in both the hadronic and the photonic cases. Starting from the usual $\overline{\text{MS}}$ scheme of fixed-order calculations [36–38,29], the transformation reads

$$\Delta C_1 = \begin{pmatrix} -C_{\gamma q,1}^{\overline{\text{MS}}}(x) & -C_{\gamma g,1}^{\overline{\text{MS}}}(x) \\ C_{\gamma g,1}^{\overline{\text{MS}}}(x) & C_{\gamma g,1}^{\overline{\text{MS}}}(x) \end{pmatrix},$$

$$\Delta C_{\gamma,1} = \begin{pmatrix} -C_{\gamma\gamma,1}^{\overline{\text{MS}}}(x) \\ 0 \end{pmatrix}. \qquad (2.30)$$

The lower-row choice in the hadronic part is the conventional continuation of the sum-rule constraint to all $N$, that one of the photonic part is taken over from the $\text{DIS}_\gamma$ scheme of Ref. [32]; see also Sec. III C. This concludes the general all-order framework, and we can now turn to the resummed anomalous dimensions and coefficient functions.

## III. SMALL-$x$ RESUMMATIONS FOR THE ANOMALOUS DIMENSIONS AND COEFFICIENT FUNCTIONS

In this section we briefly summarize relations for the resummed singlet anomalous dimensions in Mellin-$N$ space which are used in the numerical analysis below. The anomalous dimension matrix is related to the corresponding singlet splitting functions by

$$\gamma(N, a_s) = -2P(N, a_s) \equiv -2 \int_0^1 dx\, x^N P(x, \alpha_s). \qquad (3.1)$$

The general form of the small-$x$ resummed, unpolarized anomalous dimension matrix reads

$$\gamma_{\text{res}}(N, a_s) = \sum_{k=0}^{\infty} \left(\frac{\bar{\alpha}_s}{N}\right)^{k+1} \sum_{m=0}^{\infty} \bar{\alpha}_s{}^m \gamma_k^{(m)}, \qquad (3.2)$$

with $\bar{\alpha}_s = C_A \alpha_s(Q^2)/\pi$. In the discussion below we include the LO [24] and NLO [27] anomalous dimensions $\gamma_0$ and $\gamma_1$ completely, and account for the small-$x$ resummed series in the leading (L$x$, $m=0$) and next-to-leading (NL$x$, $m=1$) small-$x$ approximations:

$$\gamma(N, \alpha_s) = a_s \gamma_0(N) + a_s^2 \gamma_1(N)$$
$$+ \sum_{k=2}^{\infty} \left(\frac{\bar{\alpha}_s}{N}\right)^{k+1} [\gamma_k^{(0)} + N \gamma_k^{(1)} + O(N^2)]. \qquad (3.3)$$

### A. The leading series

The all-order resummation of the L$x$ series was performed in Ref. [4]:

$$\gamma_L(N, \alpha_s) = -2 \sum_{k=0}^{\infty} \begin{pmatrix} g_{k,qq}^{(0)} & g_{k,qg}^{(0)} \\ g_{k,gq}^{(0)} & g_{k,gg}^{(0)} \end{pmatrix} \left(\frac{\bar{\alpha}_s}{N}\right)^{k+1}$$
$$= -2 \begin{pmatrix} 0 & 0 \\ C_F/C_A & 1 \end{pmatrix} \gamma_L(N, \alpha_s) \qquad (3.4)$$

with $\gamma_L(N, \alpha_s)$ being the solution of

$$\rho \equiv \frac{N}{\bar{\alpha}_s} = 2\psi(1) - \psi(\gamma_L) - \psi(1 - \gamma_L) \equiv \chi_0(\gamma_L). \qquad (3.5)$$

$\psi(z)$ denotes the logarithmic derivative of Euler's $\Gamma$-function. $\gamma_L$ is a multi-valued function for complex values of $N$. The perturbative branch of the solution is selected by the requirement [39]

$$\gamma_L(N, \alpha_s) \to \frac{\bar{\alpha}_s}{N} \quad \text{for} \quad |N| \to \infty. \qquad (3.6)$$

For small values of $\gamma_L(N, \alpha_s)$ the asymptotic representation

$$\gamma_L = \frac{\bar{\alpha}_s}{N} \left\{ 1 + 2 \sum_{l=1}^{\infty} \zeta(2l+1) \gamma_L^{2l+1} \right\} \qquad (3.7)$$

holds, from which the coefficients $g_{k,gg}^{(0)}$ in Eq. (3.4) can be determined iteratively. Here $\zeta(n)$ denotes the Riemann $\zeta$-function. Note that only $\zeta$-functions of odd integers contribute, which is expected for physical quantities in four dimensions; cf. Ref. [40]. Analytic expressions for $g_{k,gg}^{(0)}$ were given up to $k = 14$ in Ref. [41]. Later both analytic representations and the numerical values of these coefficients were determined to large values of $k$ by various authors (cf., e.g., Refs. [42,43]). In fact, the series (3.4) can be used as representation of $\gamma_L(N, \alpha_s)$ along typical integration contours (cf. Fig. 4 in Sec. V) for the inverse Mellin transform, as shown in Ref. [43]: 20 terms (or less) in Eq. (3.4) are sufficient to obtain an accuracy of better than 0.01%.

For the later numerical analysis, i.e., to perform the Mellin inversion of the solution of the evolution equations, it is necessary to locate the singularities of $\gamma_L(N, \alpha_s)$ in the complex $N$ plane. The singularities of the resummed leading sin-
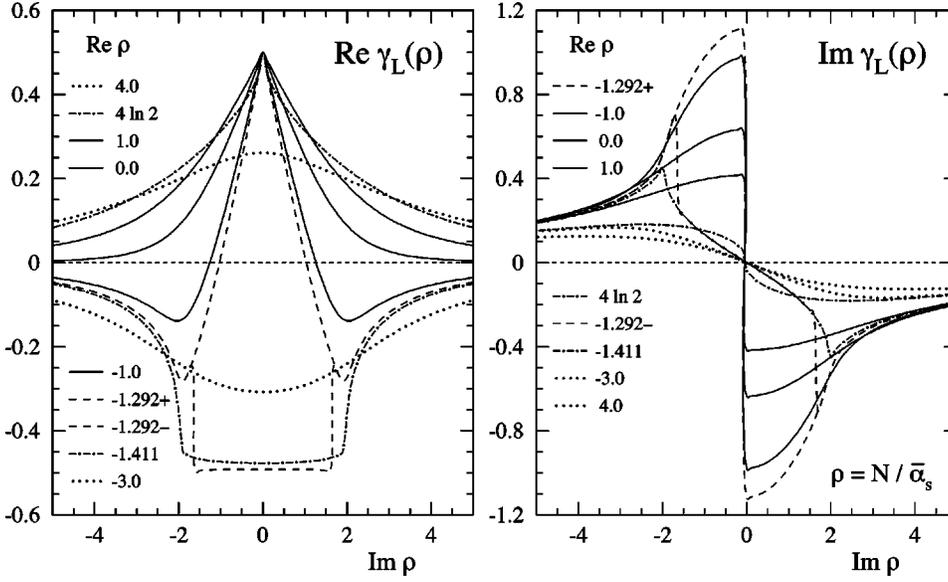
FIG. 1. The real and imaginary parts of the perturbative branch of $\gamma_L$ [4] as a function of $\rho = N/\bar{\alpha}_s$. The the dash-dotted lines are the contours through the singularities, Eq. (3.10).

gular part of the anomalous dimension $\gamma_L$ can be determined by differentiating Eq. (3.5) with respect to $\rho$:

$$\frac{d\gamma_L}{d\rho}[-\psi'(\gamma_L)+\psi'(1-\gamma_L)]=1. \tag{3.8}$$

The condition

$$\left[\frac{d\gamma_L}{d\rho}\right]^{-1}=\psi'(\gamma_L)-\frac{\pi^2}{2}\frac{1}{\sin^2(\pi\gamma_L)}=0 \tag{3.9}$$

yields the value of the resummed anomalous dimension $\gamma_L$ at the branch points. The corresponding values of $\rho$ are then determined by Eq. (3.5). For the perturbative branch one obtains

$$\gamma_1=\frac{1}{2}, \qquad \gamma_{2,3}\simeq-0.425214\pm0.473898i,$$

$$\rho_1=4\ln 2, \quad \rho_{2,3}\simeq-1.41048\pm1.97212i; \tag{3.10}$$

cf. Refs. [43,44]. The behavior of the real and imaginary parts of $\gamma_L(\rho)$ is illustrated in Fig. 1. For $\mathrm{Re}\rho\rightarrow4\ln2$, the first branch point, $\mathrm{Re}\gamma_L(\rho)$, forms a ''roof'' at $\gamma_L=1/2$ for $\mathrm{Im}\rho=0$, which remains stable over some distance in $\mathrm{Re}\rho$. The imaginary part becomes discontinuous. At smaller values of $\mathrm{Re}\rho$, $\mathrm{Re}\gamma_L(\rho)$ develops two symmetric minima, and for even smaller values two additional maxima. Both extrema finally form the two other branch points, Eq. (3.10). In $\mathrm{Im}\gamma_L$ these branch points manifest as single extrema of the corresponding curve for $\mathrm{Re}\rho=\text{const}$.

### B. Next-order corrections

The coefficients $\gamma_{qg,k}^{(1)}$ and $\gamma_{qq,k}^{(1)}$ of the NL$x$ series in Eq. (3.3) were calculated in Ref. [8]. Recently also the first terms for $\gamma_{gg,k}^{(1)}$ have been determined [9,10]. All these quantities are analytic functions of $\gamma_L$; hence they do not introduce new singularities. The energy-scale dependent contributions to $\gamma_{gg,k}^{(1)}$ have still to be derived, and the terms $\gamma_{gq,k}^{(1)}$ are also unknown so far in

$$\gamma_{\mathrm{NL}}(N,\alpha_s)\equiv\bar{\alpha}_s\sum_{k=0}^{\infty}\left(\frac{\bar{\alpha}_s}{N}\right)^k\gamma_k^{(1)}$$

$$=-2\begin{pmatrix}\dfrac{C_F}{C_A}\left[\gamma_{qg,\mathrm{NL}}-\dfrac{2}{3\pi}\alpha_s T_F\right] & \gamma_{qg,\mathrm{NL}}\\[2ex]\gamma_{gq,\mathrm{NL}} & \gamma_{gg,\mathrm{NL}}\end{pmatrix}_{\mathrm{DIS}}. \tag{3.11}$$

In the DIS factorization scheme, the function $\gamma_{qg,\mathrm{NL}}(N,\alpha_s)$ is given by

$$\gamma_{qg,\mathrm{NL}}^{\mathrm{DIS}}(N,\alpha_s)$$

$$=\gamma_{qg,\mathrm{NL}}^{Q_0}(N,\alpha_s)R(\gamma_L)$$

$$=T_F\frac{\alpha_s}{6\pi}\frac{2+3\gamma_L-3\gamma_L^2}{3-2\gamma_L}\frac{[B(1-\gamma_L,1+\gamma_L)]^3}{B(2+2\gamma_L,2-2\gamma_L)}R(\gamma_L)$$

$$\equiv\frac{2\alpha_s}{3\pi}T_F\sum_{k=0}^{\infty}g_{k,qg}^{(1)}\left(\frac{\bar{\alpha}_s}{N}\right)^k \tag{3.12}$$

with

$$R(\gamma)=\left[\frac{\Gamma(1-\gamma)\chi_0(\gamma)}{\Gamma(1+\gamma)\{-\gamma\chi_0'(\gamma)\}}\right]^{1/2}$$

$$\times\exp\left[\gamma\psi(1)+\int_0^{\gamma}d\zeta\frac{\psi'(1)-\psi'(1-\zeta)}{\chi_0(\zeta)}\right]$$

$$\equiv\sum_{k=0}^{\infty}r_k\left(\frac{\bar{\alpha}_s}{N}\right)^k. \tag{3.13}$$
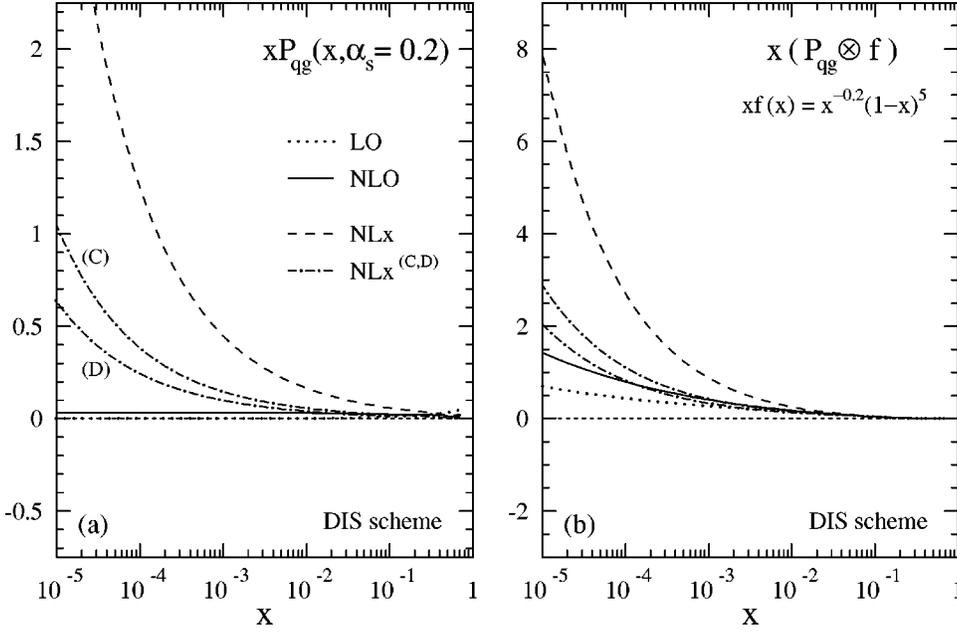
FIG. 2. (a) The cumulative effect of the available contributions on the splitting function $xP_{qg}(x)$ for $\alpha_s = 0.2$. The fixed-order results are supplemented by the small-$x$ resummed NL$x$ corrections [8] beyond NLO. Also shown are the modifications induced by the subleading terms (C) and (D) of Sec. IV. (b) As in (a) but for the convolution of $P_{qg}$ with a typical shape of an hadronic gluon density.

Here $B(x,y)$ denotes Euler's Beta-function, and $\gamma_{ij,\mathrm{NL}}^{Q_0}$ represents the anomalous dimensions in the $Q_0$-scheme [45], in which the factor $R(\gamma_L)$ does not appear.

The presently available contributions to the splitting function $xP_{qg}(x)$ in the DIS scheme and their convolutions with a typical gluon shape are shown in Fig. 2 for $\alpha_s = 0.2$, i.e., $Q^2 \simeq 20$ GeV$^2$. The LO splitting function vanishes like $x$ for $x \to 0$; their NLO counterpart is constant for $x \to 0$. The strongly rising NL$x$ result [8] therefore dominates below $x \sim 10^{-2}$. This dominance persists after the convolution below $x \sim 10^{-3}$, although here the differences are considerably smaller than for the splitting functions themselves.

The contributions $\propto N_f$ [9,46–48] and the energy-scale independent terms $\propto C_A$ [10,47] of $\gamma_{gg,\mathrm{NL}}(N,\alpha_s)$ (cf. also [49]) have been calculated recently. As shown in Ref. [9], $\gamma_{gg,\mathrm{NL}}(N,\alpha_s)$ can be obtained from the larger eigenvalue $\gamma_+$ of the resummed anomalous dimension matrix

$$\gamma_\pm = \frac{1}{2}(\gamma_{qq} + \gamma_{gg}) \pm \frac{1}{2}\sqrt{(\gamma_{gg} - \gamma_{qq})^2 + 4\gamma_{qg}\gamma_{gq}}, \qquad (3.14)$$

where

$$\gamma_+ \simeq \gamma_{gg} + \frac{\gamma_{qg}\gamma_{gq}}{\gamma_{gg} - \gamma_{qq}} = \gamma_{gg} + \frac{C_F}{C_A}\gamma_{qg} + O(\alpha_s^2 f(\bar{\alpha}_s/N)),$$

$$\gamma_- \simeq \gamma_{qq} - \frac{\gamma_{qg}\gamma_{gq}}{\gamma_{gg} - \gamma_{qq}} = \gamma_{qq} - \frac{C_F}{C_A}\gamma_{qg} + O(\alpha_s^2 f(\bar{\alpha}_s/N)).$$
$$(3.15)$$

These relations result from the fact that the quarkonic (upper-row) entries in Eq. (3.4) vanish, unlike the gluonic ones. Furthermore, one has $\gamma_- \simeq -(C_F/C_A)(2\alpha_s)/(3\pi)T_F$ due to Eq. (3.11). In the $Q_0$ scheme, the present contributions to $\gamma_+$ are determined as the solution of [9,10]

$$1 = \frac{\bar{\alpha}_s}{N}[\chi_0(\gamma_+) + \alpha_s\chi_1(\gamma_+)], \qquad (3.16)$$

which yields

$$\gamma_+^{(1)} = -\alpha_s\frac{\chi_1(\gamma_L)}{\chi_0'(\gamma_L)} \qquad (3.17)$$

after a perturbative expansion. Finally $\chi_1(\gamma)$ reads

$$\chi_1(\gamma) = \chi_1^{q\bar{q},\mathrm{a}}(\gamma) + \chi_1^{q\bar{q},\mathrm{na}}(\gamma) + \chi_1^{gg}(\gamma), \qquad (3.18)$$

with

$$\alpha_s\chi_1^{q\bar{q},\mathrm{a}} = \frac{N_f\alpha_s}{\pi}\frac{C_F}{C_A}\left(\frac{\pi}{\sin(\pi\gamma)}\right)^2\frac{\cos(\pi\gamma)}{3-2\gamma}\frac{2+3\gamma(1-\gamma)}{(1-2\gamma)(1+2\gamma)}$$

$$\alpha_s\chi_1^{q\bar{q},\mathrm{na}} = \frac{N_f\alpha_s}{6\pi}\left[\frac{1}{2}[\chi_0^2(\gamma) + \chi_0'(\gamma)] - \frac{5}{3}\chi_0(\gamma)\right.$$

$$\left. - \left(\frac{\pi}{\sin(\pi\gamma)}\right)^2\frac{3\cos(\pi\gamma)}{2(1-2\gamma)}\frac{2+3\gamma(1-\gamma)}{(1+2\gamma)(3-2\gamma)}\right]$$

$$\alpha_s\chi_1^{gg} = \frac{C_A\alpha_s}{4\pi}\left[-\frac{11}{6}[\chi_0^2(\gamma) + \chi_0'(\gamma)] + \left(\frac{67}{9} - \frac{\pi^2}{3}\right)\chi_0(\gamma)\right.$$

$$+ \left(6\zeta(3) + \frac{\pi^2}{3\gamma(1-\gamma)} + \tilde{h}(\gamma)\right)$$

$$\left. - \left(\frac{\pi}{\sin(\pi\gamma)}\right)^2\frac{\cos(\pi\gamma)}{3(1-2\gamma)}\left(11 + \frac{\gamma(1-\gamma)}{(1+2\gamma)(3-2\gamma)}\right)\right].$$
$$(3.19)$$

The function $\tilde{h}(\gamma)$ in Eq. (3.19), which contributes to $\gamma_{k,gg}^{(1)}$ only for $k \geq 2$, is given by

$$\tilde{h}(\gamma) \simeq \sum_{l=1}^{3} a_l \left( \frac{1}{l+\gamma} + \frac{1}{1+l+\gamma} \right) \qquad (3.20)$$

in approximate form, with $a_1 = 0.72$, $a_2 = 0.28$ and $a_3 = 0.16$ [10]. From these results the $Q_0$-scheme anomalous dimension is then inferred by [9]

$$\tilde{\gamma}_{gg}^{(1),Q_0} = \gamma_{gg}^{(1)} - \frac{\beta_0}{4\pi} \alpha_s^2 \frac{d}{d\alpha_s} \ln[\gamma_{gg}^{(0)} \sqrt{-\chi_0'(\gamma_{gg}^{(0)})}]$$

$$= \gamma_+^{(1)} - \frac{C_F}{C_A} \gamma_{qg}^{(1)}. \qquad (3.21)$$

Using the transformation of $\gamma_+$ to the DIS scheme [9], and employing Eqs. (3.12) and (3.15) as well, one finally arrives at

$$\gamma_{gg,\mathrm{NL}}^{\mathrm{DIS}} = \gamma_{gg,\mathrm{NL}}^{Q_0} + \frac{\beta_0}{4\pi} \alpha_s^2 \frac{d\ln R(\gamma_L)}{d\alpha_s} + \frac{C_F}{C_A} [1 - R(\gamma_L)] \gamma_{qg,\mathrm{NL}}^{Q_0}$$

$$\equiv \frac{\alpha_s}{6\pi} \sum_{k=0}^{\infty} [N_f\, g_{k,gg}^{q\bar{q},(a)} + g_{k,gg}^{q\bar{q},(b)} + \Delta g_{k,gg}^{gg}] \left( \frac{\bar{\alpha}_s}{N} \right)^k. \qquad (3.22)$$

The first terms for $\tilde{\gamma}_{gg,\mathrm{NL}}^{q\bar{q},Q_0}$ read

$$\tilde{\gamma}_{gg,\mathrm{NL}}^{q\bar{q},Q_0} = -\frac{N_f \alpha_s}{6\pi} \Bigg\{ 1 + \frac{23}{6} \frac{\bar{\alpha}_s}{N} + \left[ \frac{71}{18} - \frac{\pi^2}{6} \right] \left( \frac{\bar{\alpha}_s}{N} \right)^2 + \left[ \frac{233}{27} - \frac{13}{36} \pi^2 - 8\zeta(3) \frac{C_F}{C_A} \right] \left( \frac{\bar{\alpha}_s}{N} \right)^3$$

$$+ \left[ \frac{1276}{81} - \frac{71}{108} \pi^2 + \frac{79}{3} \zeta(3) - \frac{7}{120} \pi^4 - \frac{52}{3} \zeta(3) \frac{C_F}{C_A} \right] \left( \frac{\bar{\alpha}_s}{N} \right)^4$$

$$+ \left[ \left( \frac{8384}{243} - \frac{233}{162} \pi^2 + \frac{284}{9} \zeta(3) - \frac{91}{720} \pi^4 + 2\zeta(5) - \frac{4}{3} \zeta(3)\pi^2 \right) + \left( \frac{4}{3} \zeta(3)\pi^2 - \frac{284}{9} \zeta(3) - 16\zeta(5) \right) \frac{C_F}{C_A} \right] \left( \frac{\bar{\alpha}_s}{N} \right)^5$$

$$+ \left[ \left( \frac{45928}{729} - \frac{638}{243} \pi^2 - \frac{65}{18} \zeta(3)\pi^2 - 2\zeta(3)^2 - \frac{497}{2160} \pi^4 + \frac{125}{3} \zeta(5) + \frac{2330}{27} \zeta(3) - \frac{31}{3024} \pi^6 \right) \right.$$

$$\left. + \left( \frac{26}{9} \pi^2 \zeta(3) - \frac{104}{3} \zeta(5) - \frac{1864}{27} \zeta(3) - 80\zeta(3)^2 \right) \frac{C_F}{C_A} \right] \left( \frac{\bar{\alpha}_s}{N} \right)^6 + O\left( \frac{\bar{\alpha}_s}{N} \right)^7 \Bigg\}. \qquad (3.23)$$

A similar expression can be derived for $\gamma_{gg,\mathrm{NL}}^{gg,Q_0}$. Because of the yet approximate expression for $\tilde{h}(\gamma)$ and the missing energy-scale dependent terms, we only list the numerical values of those still preliminary expansion coefficients in Table I.

In Fig. 3 the different approximations to the splitting function $xP_{gg}(x)$ are displayed. Here both the LO and the NLO terms are flat for $x \to 0$, while the L$x$ contribution [4] causes a strong rise as $x \to 0$. Also shown are the presently known NL$x$ terms just discussed. The addition of the quarkonic (NL$x_{q\bar{q}}$) contribution [9] reduces the resummation effect almost down to the fixed-order results. The energy-scale independent gluonic terms [10] have an even stronger impact; in fact, they turn $xP_{gg}$ negative already at $x \sim 10^{-2}$ for $\alpha_s \sim 0.2$. A similar, but milder pattern is observed for the convolution $x(P_{gg} \otimes f)$ with a typical gluon shape which illustrates the $Q^2$-slope of the gluon density induced by $P_{gg}$. Note that the energy-scale dependent contributions to the NL$x$ terms in $P_{gg}$ have still to be calculated. These terms or yet unknown higher-order (NNL$x$) contributions may change the present behavior of $P_{gg}(x)$.

The leading singular contributions to the gluonic and pure-singlet quarkonic coefficient functions for the longitudinal structure function were also determined in Ref. [8],

$$C_L^g = \frac{\alpha_s}{3\pi} T_F \left( \frac{1-\gamma_L}{3-2\gamma_L} \right) \frac{[B(1-\gamma_L, 1+\gamma_L)]^3}{B(2-2\gamma_L, 2+2\gamma_L)} R(\gamma_L)$$

$$\equiv \frac{2\alpha_s}{3\pi} T_F \sum_{k=1}^{\infty} c_k^L \left( \frac{\bar{\alpha}_s}{N} \right)^k, \qquad (3.24)$$

$$C_L^S = \frac{C_F}{C_A} \left[ C_L^g - \frac{2\alpha_s}{3\pi} T_F \right]. \qquad (3.25)$$

The numerical values of the first 20 expansion coefficients $g_{k,gg}^{(0)}, g_{k,qg}^{(1)}$ in the DIS and $Q_0$ schemes, $r_k, c_k^L$, and coefficients contributing to $g_{k,gg}^{q\bar{q}}$ and $\Delta g_{k,gg}^{gg}$ are listed in Table I for completeness. These coefficients were calculated using the MAPLE package [50]. The numerical values of $g_{k,qg}^{(1)}/(4\ln 2)^k$ were tabulated before for the DIS [42] and $\overline{\mathrm{MS}}$ schemes [51]. With a low number of digits the values of $g_{k,qg}^{\overline{\mathrm{MS}},(1)}$, $r_k$ and $c_k^L$ were given in Ref. [52] as well. Either the direct expressions (3.4),(3.12) or relations based on the corresponding expansion coefficients have been previously used in numerical studies [44,23,53].

### C. Photon-parton splitting functions

Finally we have to consider the small-$x$ higher-order corrections to the inhomogeneous terms $k_q \equiv P_{q\gamma}$ and $k_g \equiv P_{g\gamma}$

TABLE I. The numerical expansion coefficients in Eqs. (3.4), (3.12), (3.13), (3.22) and (3.24).

| $k$ | $g^{(0)}_{k,gg}$ | $g^{(1)}_{k,qg}$ ($Q_0$) | $g^{(1)}_{k,qg}$ (DIS) | $r_k$ | $c^L_k$ |
|---|---|---|---|---|---|
| 0 | $1.00000 \times 10^0$ | $1.00000 \times 10^0$ | $1.00000 \times 10^0$ | $1.00000 \times 10^0$ | $1.00000 \times 10^0$ |
| 1 | $0.00000 \times 10^0$ | $2.16667 \times 10^0$ | $2.16667 \times 10^0$ | $0.00000 \times 10^0$ | $-3.33333 \times 10^{-1}$ |
| 2 | $0.00000 \times 10^0$ | $2.29951 \times 10^0$ | $2.29951 \times 10^0$ | $0.00000 \times 10^0$ | $2.13284 \times 10^0$ |
| 3 | $2.40411 \times 10^1$ | $5.06561 \times 10^0$ | $8.27109 \times 10^0$ | $3.20549 \times 10^0$ | $2.27231 \times 10^0$ |
| 4 | $0.00000 \times 10^0$ | $8.79145 \times 10^0$ | $1.49249 \times 10^1$ | $-8.11742 \times 10^{-1}$ | $4.34344 \times 10^{-1}$ |
| 5 | $2.07386 \times 10^1$ | $1.90521 \times 10^1$ | $2.92268 \times 10^1$ | $4.56248 \times 10^1$ | $2.02643 \times 10^1$ |
| 6 | $1.73393 \times 10^1$ | $4.58482 \times 10^1$ | $1.02812 \times 10^2$ | $3.27070 \times 10^1$ | $2.30315 \times 10^1$ |
| 7 | $2.01670 \times 10^0$ | $9.24159 \times 10^1$ | $1.94887 \times 10^2$ | $-2.95476 \times 10^1$ | $3.46449 \times 10^1$ |
| 8 | $3.98863 \times 10^1$ | $2.31063 \times 10^2$ | $4.85100 \times 10^2$ | $1.08183 \times 10^2$ | $2.65004 \times 10^2$ |
| 9 | $1.68747 \times 10^2$ | $5.59958 \times 10^2$ | $1.52444 \times 10^3$ | $3.99588 \times 10^2$ | $3.30038 \times 10^2$ |
| 10 | $6.99881 \times 10^1$ | $1.24822 \times 10^3$ | $3.11451 \times 10^3$ | $1.33228 \times 10^2$ | $8.50371 \times 10^2$ |
| 11 | $6.61253 \times 10^2$ | $3.25381 \times 10^3$ | $8.58375 \times 10^3$ | $2.10243 \times 10^3$ | $3.90849 \times 10^3$ |
| 12 | $1.94531 \times 10^3$ | $7.93653 \times 10^3$ | $2.47571 \times 10^4$ | $5.51142 \times 10^3$ | $5.67433 \times 10^3$ |
| 13 | $1.71768 \times 10^3$ | $1.89275 \times 10^4$ | $5.47435 \times 10^4$ | $5.30316 \times 10^3$ | $1.77680 \times 10^4$ |
| 14 | $1.06433 \times 10^4$ | $4.98520 \times 10^4$ | $1.56195 \times 10^5$ | $3.85296 \times 10^4$ | $6.21982 \times 10^4$ |
| 15 | $2.55668 \times 10^4$ | $1.23011 \times 10^5$ | $4.26980 \times 10^5$ | $8.49086 \times 10^4$ | $1.07028 \times 10^5$ |
| 16 | $3.67813 \times 10^4$ | $3.06504 \times 10^5$ | $1.01111 \times 10^6$ | $1.40384 \times 10^5$ | $3.51475 \times 10^5$ |
| 17 | $1.71685 \times 10^5$ | $8.07771 \times 10^5$ | $2.89398 \times 10^6$ | $6.94998 \times 10^5$ | $1.05058 \times 10^6$ |
| 18 | $3.75379 \times 10^5$ | $2.02210 \times 10^6$ | $7.69042 \times 10^6$ | $1.44307 \times 10^6$ | $2.10341 \times 10^6$ |
| 19 | $7.36025 \times 10^5$ | $5.17873 \times 10^6$ | $1.91919 \times 10^7$ | $3.22738 \times 10^6$ | $6.80747 \times 10^6$ |

| $k$ | $g^{q\bar{q}(a)}_{k,gg}$ ($Q_0$) | $g^{q\bar{q}(b)}_{k,gg}$ ($Q_0$) | $g^{q\bar{q}(a)}_{k,gg}$ (DIS) | $g^{q\bar{q}(b)}_{k,gg}$ (DIS) | $\Delta g^{gg}_{k,gg}$ |
|---|---|---|---|---|---|
| 0 | $-1.00000 \times 10^0$ | $0.00000 \times 10^0$ | $-1.00000 \times 10^0$ | $0.00000 \times 10^0$ | $-1.65000 \times 10^1$ |
| 1 | $-3.83333 \times 10^0$ | $0.00000 \times 10^0$ | $-3.83333 \times 10^0$ | $0.00000 \times 10^0$ | $0.00000 \times 10^0$ |
| 2 | $-2.29951 \times 10^0$ | $0.00000 \times 10^0$ | $-2.29951 \times 10^0$ | $0.00000 \times 10^0$ | $1.48980 \times 10^1$ |
| 3 | $6.42072 \times 10^0$ | $-1.19004 \times 10^2$ | $-6.04506 \times 10^0$ | $3.96679 \times 10^1$ | $-2.25291 \times 10^2$ |
| 4 | $-2.59764 \times 10^1$ | $0.00000 \times 10^0$ | $-2.81814 \times 10^1$ | $-5.35750 \times 10^1$ | $2.42631 \times 10^0$ |
| 5 | $5.75787 \times 10^0$ | $-3.42186 \times 10^2$ | $-2.60988 \times 10^1$ | $3.42186 \times 10^1$ | $-2.09481 \times 10^2$ |
| 6 | $1.21690 \times 10^2$ | $-2.28879 \times 10^3$ | $-9.43607 \times 10^1$ | $4.40583 \times 10^2$ | $-2.78211 \times 10^3$ |
| 7 | $-2.66365 \times 10^2$ | $-6.98786 \times 10^2$ | $-3.54981 \times 10^2$ | $-7.39527 \times 10^2$ | $-2.70970 \times 10^2$ |
| 8 | $5.43807 \times 10^2$ | $-1.11881 \times 10^4$ | $-4.27828 \times 10^2$ | $1.11801 \times 10^3$ | $-7.53012 \times 10^3$ |
| 9 | $1.96852 \times 10^3$ | $-4.10835 \times 10^4$ | $-1.67366 \times 10^3$ | $4.86665 \times 10^3$ | $-3.82351 \times 10^4$ |
| 10 | $-2.04998 \times 10^3$ | $-3.39345 \times 10^4$ | $-5.21390 \times 10^3$ | $-9.10195 \times 10^3$ | $-1.56381 \times 10^4$ |
| 11 | $1.49302 \times 10^4$ | $-2.75933 \times 10^5$ | $-7.99079 \times 10^3$ | $2.40902 \times 10^4$ | $-1.73122 \times 10^5$ |
| 12 | $3.33837 \times 10^4$ | $-7.55104 \times 10^5$ | $-3.05607 \times 10^4$ | $5.32758 \times 10^4$ | $-5.68231 \times 10^5$ |
| 13 | $9.19579 \times 10^3$ | $-1.10387 \times 10^6$ | $-8.37332 \times 10^4$ | $-9.58437 \times 10^4$ | $-5.13392 \times 10^5$ |
| 14 | $3.35804 \times 10^5$ | $-6.12763 \times 10^6$ | $-1.57171 \times 10^5$ | $4.46747 \times 10^5$ | $-3.52577 \times 10^6$ |
| 15 | $6.26484 \times 10^5$ | $-1.45966 \times 10^7$ | $-5.64262 \times 10^5$ | $5.92510 \times 10^5$ | $-9.13527 \times 10^6$ |
| 16 | $9.72892 \times 10^5$ | $-3.01102 \times 10^7$ | $-1.43675 \times 10^6$ | $-6.85258 \times 10^5$ | $-1.36171 \times 10^7$ |
| 17 | $7.05626 \times 10^6$ | $-1.30018 \times 10^8$ | $-3.14592 \times 10^6$ | $7.71985 \times 10^6$ | $-6.85495 \times 10^7$ |
| 18 | $1.29507 \times 10^7$ | $-2.96814 \times 10^8$ | $-1.05144 \times 10^7$ | $7.22515 \times 10^6$ | $-1.58648 \times 10^8$ |
| 19 | $3.18568 \times 10^7$ | $-7.45406 \times 10^8$ | $-2.59548 \times 10^7$ | $2.95797 \times 10^6$ | $-3.23625 \times 10^8$ |

in the photonic evolution equations (2.21). These quantities arise from a subset of the diagrams leading to the gluon-parton splitting functions, with the incoming gluon replaced by a photon. Purely gluonic graphs do obviously not belong to that subset, as the photon can couple to the hadronic system only through $q\bar{q}$ emission. Hence, by comparing to the hadronic results discussed above, one obtains the most singular ($S$) small-$x$ terms as

$$k^S_q = a_{\rm em} k_{q,0}(N=0) + \sum_{l=1}^{\infty} a_{\rm em} a^l_s \frac{k^S_{q,0}}{N^{l-1}},$$

$$k^S_g = \sum_{l=1}^{\infty} a_{\rm em} a^l_s \frac{k^S_{g,0}}{N^l}. \tag{3.26}$$

I.e., $k_q$ (up to its scheme-independent constant LO term) is
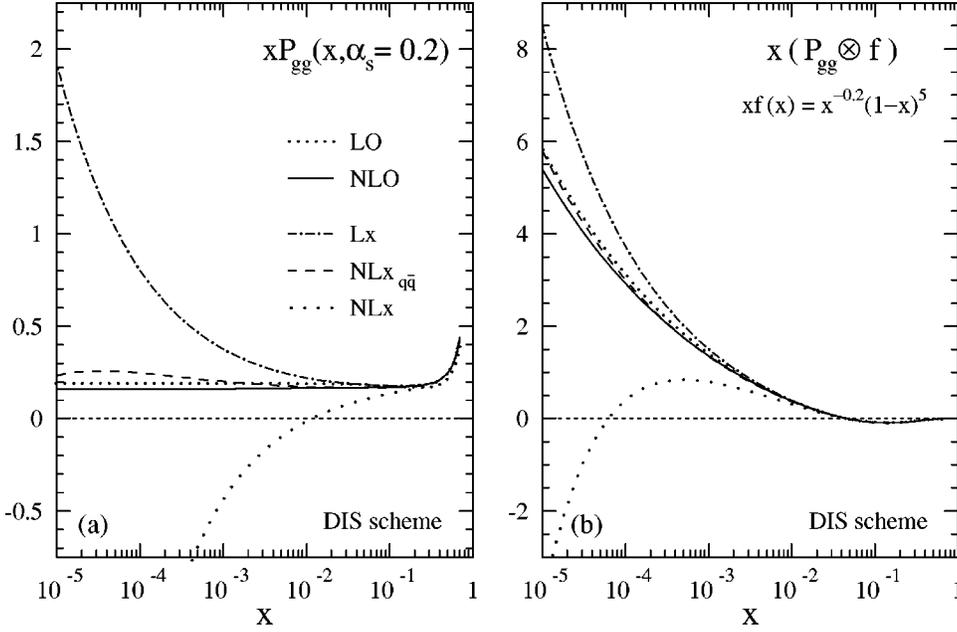
FIG. 3. (a) The cumulative effect of the available terms for splitting function $xP_{gg}(x)$ for $\alpha_s = 0.2$. The fixed-order results are successively supplemented by the higher-order small-$x$ resummed L$x$ correction [4], the $q\bar{q}$ contribution to the NL$x$ term [9], and the gluonic NL$x$ energy-scale independent terms [10]. (b) As (a) but for the convolution of $P_{gg}$ with a shape of an hadronic gluon density.

definitely beyond the current NL$x$ approximation, whereas $k_g$ can receive contributions at this order. Likewise, the constant but scheme-dependent term $C_{\gamma,1}$ is NL$x$, and all higher-order photonic coefficient functions are beyond that approximation. A $1/N$-term is indeed present in the known NLO result $k_{g,1}$. This term, however, vanishes after transformation to the DIS or DIS$_\gamma$ schemes. In fact, this cancellation can always be achieved at all orders, as we will show now.

We proceed in two steps. We start by a purely hadronic transformation (like that one from $\overline{\text{MS}}$ to DIS), where $\boldsymbol{C} \rightarrow \widetilde{\boldsymbol{C}} = \boldsymbol{C} + \Delta\boldsymbol{C}$, and $\boldsymbol{C}_\gamma$ remains unchanged. Then Eq. (2.27) implies

$$0 = \Delta\boldsymbol{I}_{\text{inhom}} = \widetilde{\boldsymbol{C}} \cdot \Delta\boldsymbol{k} + \Delta\boldsymbol{C} \cdot \boldsymbol{k}. \qquad (3.27)$$

We consider only such transformation terms, which are motivated in contributions to the actual electromagnetic coefficient functions. These are, however, of NL$x$ order, as the $\boldsymbol{k}$ themselves, and hence one has $\Delta\boldsymbol{k} = 0$ on the NL$x$ level: purely hadronic scheme changes modify the photon-parton splitting functions only beyond the NL$x$ approximation.

The second step is a purely photonic transformation, $\boldsymbol{C}_\gamma \rightarrow \widetilde{\boldsymbol{C}}_\gamma = \boldsymbol{C}_\gamma + \Delta\boldsymbol{C}_\gamma$, with $\boldsymbol{C}$ untouched. Here Eq. (2.27) yields

$$0 = \Delta\boldsymbol{I}_{\text{inhom}} = \boldsymbol{C} \cdot \Delta\boldsymbol{k} + \beta \cdot \Delta\boldsymbol{C}'_\gamma - \boldsymbol{I}_{\text{hom}} \cdot \Delta\boldsymbol{C}_\gamma. \qquad (3.28)$$

Solving for the changes $\Delta\boldsymbol{k}_m$ up to the order $a_{\text{em}} a_s^m$ therefore leads to

$$\Delta\boldsymbol{k}_1 = \boldsymbol{I}_{\text{hom},0} \cdot \Delta\boldsymbol{C}_{\gamma,1}$$

$$\Delta\boldsymbol{k}_2 = -\boldsymbol{C}_1 \cdot \Delta\boldsymbol{k}_1 + \boldsymbol{I}_{\text{hom},0} \cdot \Delta\boldsymbol{C}_{\gamma,2} + \boldsymbol{I}_{\text{hom},1} \cdot \Delta\boldsymbol{C}_{\gamma,1}$$

$$\vdots$$

$$\Delta\boldsymbol{k}_m = -\sum_{l=1}^{m-1} \boldsymbol{C}_l \cdot \Delta\boldsymbol{k}_{m-l} + \sum_{l=0}^{m-1} \boldsymbol{I}_{\text{hom},l} \cdot \Delta\boldsymbol{C}_{\gamma,m-l+1}, \qquad (3.29)$$

where only terms have been retained which can potentially contribute to $\Delta\boldsymbol{k}_{\text{NL}x}$, if an NL$x$ contribution to $\Delta\boldsymbol{C}_\gamma$ occurs in the transformation. By choice of the (unphysical) lower component of $\underline{\Delta\boldsymbol{C}_{\gamma,m}}$ the NL$x$ pieces of $\boldsymbol{k}_m$, arising, for example, in an $\overline{\text{MS}}$ calculation, can hence successively be eliminated, without disturbing the vanishing of the upper term. At NLO, e.g., the lower component of zero in Eq. (2.30), as chosen in the DIS$_\gamma$ scheme [32] achieves this cancellation. Therefore, without any loss of generality, vanishing resummed photon-parton splitting functions can be assumed at the NL$x$ level.

## IV. LESS SINGULAR CONTRIBUTIONS

The terms in the splitting functions $P_{ij}$, which are less singular by one (or more) powers of $\ln(1/x)$ as $x \rightarrow 0$ than the leading contributions discussed in the previous section, are presently unknown in almost all cases. Such subleading contributions, however, can potentially prove to be as important as the leading terms, as also noted in a similar context in Ref. [54]. The splitting functions and coefficient functions enter observable quantities always via Mellin convolutions with the parton distributions. Since the parton densities are steeply rising towards small $x$, but (at least in the hadronic case) small at large $x$, the structure functions probe the behavior of splitting functions and coefficient functions at medium and large values of $x$ as well.

The unpolarized singlet splitting functions are constrained by energy-momentum conservation; see Eq. (2.17). Also in other cases, however, as for the polarized singlet and the non-singlet $+$ evolutions, where no conservation laws apply, less singular terms with sizable coefficients exist, for example in NLO; see, e.g., Ref. [23]. In order to evaluate the possible impact of such terms in higher-order splitting functions, their numerical coefficients need to be estimated. At present the almost only source of information is the fully known LO and NLO splitting functions.

The dominant and subdominant terms in the small-$x$ $1/N$-expansion of the LO and NLO singlet anomalous dimensions are recalled in Eqs. (4.1)–(4.3). In accordance with the main part of our numerical studies in Sec. VI, the results are listed for four light quark flavors. The first terms in the LO case are given by

$$\gamma_{qq,\text{LO}} = +10.8793N - 6.82222N^2 + O(N^3),$$

$$\gamma_{qg,\text{LO}} = -10.6667 + 11.5556N - 13.1852N^2 + O(N^3),$$

$$\gamma_{gq,\text{LO}} = -\frac{10.6667}{N} + 8.00000 - 9.3333N$$
$$+ 10.0000N^2 + O(N^3),$$

$$\gamma_{gg,\text{LO}} = -\frac{24.0000}{N} + 27.3333 - 5.1883N$$
$$+ 17.0395N^2 + O(N^3). \tag{4.1}$$

The corresponding expansions of the NLO anomalous dimensions read, in the DIS scheme,

$$\gamma_{qq,\text{NLO}}^{\text{DIS}} = -\frac{123.259}{N} + 405.863 - 684.836N$$
$$+ 1197.52N^2 + O(N^3),$$

$$\gamma_{qg,\text{NLO}}^{\text{DIS}} = -\frac{277.333}{N} + 846.222 - 1706.18N$$
$$+ 2622.76N^2 + O(N^3),$$

$$\gamma_{gq,\text{NLO}}^{\text{DIS}} = +\frac{91.2593}{N} - 453.512 + 809.030N$$
$$- 1344.89N^2 + O(N^3),$$

$$\gamma_{gg,\text{NLO}}^{\text{DIS}} = +\frac{245.333}{N} - 988.210 + 2093.25N$$
$$- 3109.08N^2 + O(N^3). \tag{4.2}$$

One notices that the first subleading terms occur with a sign opposite to that of the dominant one. Their prefactors are of the same order, but in most cases the subleading coefficients are by a factor of about 2–4 larger. At leading order the quarkonic terms are not singular as $N \to 0$. The $qq$-term even starts proportional to $N$, as a consequence of fermion-number conservation, Eq. (2.16). The alternating structure continues towards higher powers in $N$ with a similar pattern for the coefficients as observed for the first and second terms. Note that this behavior is not a special feature

of the DIS scheme, but is observed to a similar extent also in other schemes. As an example we give the corresponding coefficients also for the $\overline{\text{MS}}$-scheme :

$$\gamma_{qq,\text{NLO}}^{\overline{\text{MS}}} = -\frac{94.8148}{N} + 253.026 - 337.185N$$
$$+ 623.259N^2 + O(N^3),$$

$$\gamma_{qg,\text{NLO}}^{\overline{\text{MS}}} = -\frac{213.333}{N} + 461.449 - 889.687N$$
$$+ 1501.16N^2 + O(N^3),$$

$$\gamma_{gq,\text{NLO}}^{\overline{\text{MS}}} = +\frac{62.8148}{N} - 361.805 + 658.108N$$
$$- 1048.43N^2 + O(N^3),$$

$$\gamma_{gg,\text{NLO}}^{\overline{\text{MS}}} = +\frac{216.889}{N} - 790.928 + 1616.55N$$
$$- 2423.77N^2 + O(N^3). \tag{4.3}$$

In the structure function evolution, the difference between Eqs. (4.2) and (4.3) is compensated by the corresponding small-$x$ terms of the coefficient functions.

In the small-$x$ resummation case, even partial results for subdominant contributions are only available for the gluon-gluon splitting function so far. The irreducible NL$x$ contributions to $\gamma_{gg}$ [10] exhibit very large coefficients if compared to the L$x$ series [4]; see Table I and the comparison in Ref. [12]. The introduction of terms with prefactors up to 2 times larger than those of the leading contributions, therefore, should provide conservative, non-exaggerating estimates for the possible impact of subdominant corrections. The following modifications of the resummed anomalous dimensions beyond two-loop order, $\Gamma(N, \alpha_s)$, have accordingly been studied within Refs. [21,23,44,55]:

$$\text{(A):} \quad \Gamma(N, \alpha_s) \to \Gamma(N, \alpha_s) - \Gamma(1, \alpha_s)$$

$$\text{(B):} \quad \Gamma(N, \alpha_s) \to \Gamma(N, \alpha_s)(1 - N)$$

$$\text{(C):} \quad \Gamma(N, \alpha_s) \to \Gamma(N, \alpha_s)(1 - N)^2$$

$$\text{(D):} \quad \Gamma(N, \alpha_s) \to \Gamma(N, \alpha_s)(1 - 2N + N^3). \tag{4.4}$$

The impact of the prescriptions (C) and (D) on the resummed NL$x$ contribution to the splitting function $xP_{qg}(x, \alpha_s)$ is illustrated in Fig. 2. At $x = 10^{-4}$ those terms reduce $xP_{qg}$ by factors larger than 3, indicating the potential importance of less singular contributions. Also displayed in Fig. 2 is the convolution of $P_{qg}$ with a typical hadronic gluon shape. The enhancement of the importance of non-leading terms by the Mellin convolution discussed above is obvious from the comparison of the two plots.

## V. SOLUTION OF THE EVOLUTION EQUATIONS

In this section we derive the solution of the singlet evolution equations presented above. For technical convenience the analysis is performed in Mellin-$N$ space where the convolutions turn to simple products. Recall that a unique analytic continuation of the anomalous dimensions from the integer moments to complex $N$ exists [56]. Thus a coupled system of two ordinary differential equations has to be solved at fixed $N$. The $x$-space results are then obtained by a contour integral around the singularities of the final moment solutions $f(N)$ in the complex $N$-plane, e.g., that shown in Fig. 4. Because of $f^*(N) = f(N^*)$, it yields [57]

$$x f(x) = \frac{1}{\pi} \int_0^\infty dz \; \mathrm{Im}[e^{i\phi} x^{-C} f(N=C)], \qquad (5.1)$$

where $C = c + z e^{i\phi}$. For all cases considered here, $c \simeq 1$ and $\phi \simeq 3\pi/4$ provide an efficient and numerically stable inversion. The latter choice of $\phi > \pi/2$ leads to a faster convergence of the integral (5.1) as $z \to \infty$; see also Ref. [58]. At small-$x$, for example, a numerical accuracy better than $10^{-5}$ is easily achieved for upper limits as low as $z_{\mathrm{max}} \simeq 5$.
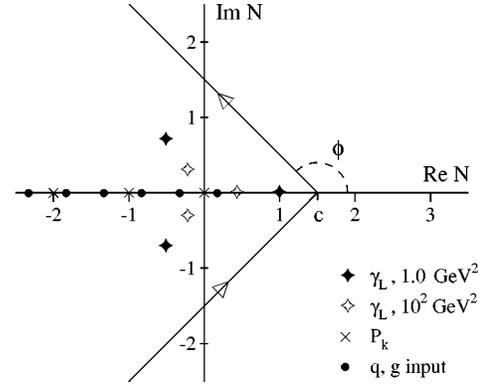


FIG. 4. Integration contour in the complex $N$-plane for the inverse Mellin transformation (5.1) relative to the locations of the singularities of typical initial parton distributions (solid circles), and those of the fixed-order (crosses) and resummed anomalous dimensions (open and solid diamonds for different values of $Q^2$).

### A. The general hadronic solution

It is convenient to recast the evolution equations in terms of the running coupling $a_s = \alpha_s(Q^2)/4\pi$ as independent variable, by combining the $Q^2$ evolution (2.14) of the hadronic parton densities $q$ with Eq. (2.8) for $a_s$. Sorting the resulting right-hand side (RHS) in powers of $a_s$, one obtains

$$\frac{\partial \boldsymbol{q}(a_s, N)}{\partial a_s} = \frac{a_s \boldsymbol{P}_0(N) + a_s^2 \boldsymbol{P}_1(N) + a_s^3 \boldsymbol{P}_2(N) + \cdots}{-a_s^2 \beta_0 - a_s^3 \beta_1 - a_s^4 \beta_2 - \cdots} \boldsymbol{q}(a_s, N)$$

$$= -\frac{1}{\beta_0 a_s}\left( \boldsymbol{P}_0(N) + a_s\left( \boldsymbol{P}_1(N) - \frac{\beta_1}{\beta_0}\boldsymbol{P}_0(N) \right) + a_s^2\left\{ \boldsymbol{P}_2(N) - \frac{\beta_1}{\beta_0}\boldsymbol{P}_1(N) + \left[ \left(\frac{\beta_1}{\beta_0}\right)^2 - \frac{\beta_2}{\beta_0} \right]\boldsymbol{P}_0(N) \right\} + \cdots \right) \boldsymbol{q}(a_s, N)$$

$$= -\frac{1}{a_s}\left[ \boldsymbol{R}_0(N) + \sum_{k=1}^{\infty} a_s^k \boldsymbol{R}_k(N) \right] \boldsymbol{q}(a_s, N). \qquad (5.2)$$

Here we have simplified the notation by introducing the recursive abbreviations

$$\boldsymbol{R}_0 \equiv \frac{1}{\beta_0}\boldsymbol{P}_0, \qquad (5.3)$$

$$\boldsymbol{R}_k \equiv \frac{1}{\beta_0}\boldsymbol{P}_k - \sum_{i=1}^{k} \frac{\beta_i}{\beta_0}\boldsymbol{R}_{k-i} \qquad (5.4)$$

for the splitting function combinations entering this expansion. As in Eqs. (5.3) and (5.4), we will often suppress the explicit reference to the Mellin variable $N$ below.

The splitting function matrices $\boldsymbol{P}_k$ of different orders $k$ do generally not commute; especially one has

$$[\boldsymbol{R}_{k \geqslant 1}(N), \boldsymbol{R}_0(N)] \neq 0. \qquad (5.5)$$

This prevents, already at NLO, writing the solution of Eq. (5.2) in a closed exponential form. Instead we proceed by generalizing the NLO method of Ref. [33] to all orders[4] in $a_s$. The corresponding *Ansatz* of a series expansion around the lowest order solution,

$$\boldsymbol{q}^{\mathrm{LO}}(a_s, N) = \left( \frac{a_s}{a_0} \right)^{-\boldsymbol{R}_0(N)} \boldsymbol{q}(a_0, N) \equiv \boldsymbol{L}(a_s, a_0, N)\boldsymbol{q}(a_0, N), \qquad (5.6)$$

reads

––––––––
[4]The first three orders were treated in a very similar manner in Ref. [59].

$$q(a_s,N)=U(a_s,N)L(a_s,a_0,N)U^{-1}(a_0,N)q(a_0,N)$$

$$=\left[1+\sum_{k=1}^{\infty}a_s^kU_k(N)\right]L(a_s,a_0,N)$$

$$\times\left[1+\sum_{k=1}^{\infty}a_0^kU_k(N)\right]^{-1}q(a_0,N). \qquad (5.7)$$

The third, $a_s$-independent factor in Eq. (5.7) has been introduced to normalize the evolution operator to the unit matrix at $Q_0^2$, instead of to the LO result (5.6) at infinitely high $Q^2$. Inserting this *Ansatz* into the evolution equations (5.2) and sorting in powers of $a_s$ anew, one arrives at a chain of commutation relations for the expansion coefficients $U_k(N)$:

$$[U_1,R_0]=R_1+U_1,$$

$$[U_2,R_0]=R_2+R_1U_1+2U_2,$$

$$\vdots$$

$$[U_k,R_0]=R_k+\sum_{i=1}^{k-1}R_{k-i}U_i+kU_k\equiv\tilde{R}_k+kU_k. \qquad (5.8)$$

These equations can be solved recursively by applying the eigenvalue decomposition of the LO splitting function matrix, completely analogous to the truncated NLO solution with only $U_1$ [33]; see below. One writes

$$R_0=r_-e_-+r_+e_+, \qquad (5.9)$$

where $r_-$ ($r_+$) stands for the smaller (larger) eigenvalue of $R_0$,

$$r_\pm=\frac{1}{2\beta_0}[P_{qq}^{(0)}+P_{gg}^{(0)}\pm\sqrt{(P_{qq}^{(0)}-P_{gg}^{(0)})^2+4P_{qg}^{(0)}P_{gq}^{(0)}}]. \qquad (5.10)$$

The matrices $e_\pm$ denote the corresponding projectors,

$$e_\pm=\frac{1}{r_\pm-r_\mp}[R_0-r_\mp I], \qquad (5.11)$$

with $I$ being the $2\times2$ unit matrix. Hence the LO evolution operator (5.6) can be represented as

$$L(a_s,a_0,N)=e_-(N)\left(\frac{a_s}{a_0}\right)^{-r_-(N)}+e_+(N)\left(\frac{a_s}{a_0}\right)^{-r_+(N)}. \qquad (5.12)$$

Inserting the identity

$$U_k=e_-U_ke_-+e_-U_ke_++e_+U_ke_-+e_+U_ke_+ \qquad (5.13)$$

into the commutation relations (5.8), one finally obtains the expansion coefficients in Eq. (5.7):

$$U_k=-\frac{1}{k}[e_-\tilde{R}_ke_-+e_+\tilde{R}_ke_+]+\frac{e_+\tilde{R}_ke_-}{r_--r_+-k}+\frac{e_-\tilde{R}_ke_+}{r_+-r_--k}. \qquad (5.14)$$

This relation completes the general structure of the hadronic singlet evolution. Note that the poles in $U_k(N)$ at $N$-values where $r_-(N)-r_+(N)\pm k$ vanishes are canceled by the $U^{-1}$ term in the solution (5.7). We are now ready to consider the presently available fixed-order and small-$x$ resummation approximations.

### B. Fixed-order evolution

In fixed-order perturbative QCD the expansion (2.15) of the splitting functions in powers of the strong coupling $a_s$ is truncated at some low order $k$. Practical small-$x$ calculations are presently restricted to NLO ($k=1$), as the NNLO splitting functions $P_2(N)$ are not yet known for arbitrary values of $N$, unlike the 2-loop coefficient functions [37,38] and the $\beta$-function coefficient $\beta_2$ [17]. Hence we confine ourselves to the NLO evolution here, the generalization to higher fixed orders being obvious. I.e., we keep the full results up to $k=1$ and put, in Eq. (5.2),

$$P_{k\geqslant2}(N)=0, \qquad (5.15)$$

$$\beta_{k\geqslant2}=0. \qquad (5.16)$$

The coefficients $\beta_{k\geqslant2}$ are also removed, for only all three quantities $P_k$, $C_k$ and $\beta_k$ together form a scheme independent set for the evolution of physical quantities like the structure functions $F_2(x,Q^2)$ or, in the case of polarized scattering, $g_1(x,Q^2)$.

Two natural approaches have been widely adopted for the solution of the resulting NLO evolution equations. First one can solve Eq. (5.2) as it stands after inserting Eqs. (5.15) and (5.16). Then still all orders in $a_s$ contribute there and in the solution (5.7), with the only simplification that the splitting function combinations (5.4) are now given by

$$R_k^{\text{NLO}}=\frac{(-1)^{k-1}}{\beta_0}\left(\frac{\beta_1}{\beta_0}\right)^{k-1}\left(P_1-\frac{\beta_1}{\beta_0}P_0\right). \qquad (5.17)$$

This procedure is equivalent to a simple iterative solution of the system (2.14) and (2.8), truncated at $k=1$. That technique is widely used in parton density analyses, e.g., in Refs. [60–62].

The second approach uses power counting in $a_s$ at the level of the evolution equation (5.2). There the $a_s^2$ term in the square brackets involves $P_2$ and $\beta_2$ and can thus be considered as beyond the present approximation. Consequently only the constant and the linear terms in $a_s$ are kept, instead of Eq. (5.17) leading to

$$R_1^{\text{NLO}'}=R_1^{\text{NLO}}=\frac{1}{\beta_0}\left(P_1-\frac{\beta_1}{\beta_0}P_0\right), \quad R_{k\geqslant2}^{\text{NLO}'}=0. \quad (5.18)$$

In this approach it is furthermore natural to truncate also the evolution matrix $U(a_s)$ after the linear term, since $P_2$ would enter the determination of $U_2$ in Eq. (5.8) as well. Recall also that the final multiplication with the NLO Wilson coefficients only cancels the scheme dependence of the linear $a_s$ term in the evolution of the structure functions (2.25). Fi-

nally one can expand also $U^{-1}(a_0)$ to first order in Eq. (5.7), although this is not necessary, resulting in

$$q_{\text{tr}}^{\text{NLO}}(a_s,N) = [L(a_s,a_0,N) + a_s U_1(N)L(a_s,a_0,N)$$
$$- a_0 L(a_s,a_0,N)U_1(N)]q(a_0,N), \quad (5.19)$$

where $U_1$ is given by Eq. (5.14) with $\tilde{R}_1 = R_1$ of Eq. (5.18). This is the well-known truncated analytical NLO solution [33] which has been employed, for instance, in Refs. [63,64].

These two approaches obviously differ in NNLO terms only. The former procedure introduces more scheme-dependent higher order terms into the evolution of structure functions such as $F_2(x,Q^2)$ or $g_1(x,Q^2)$ in a general factorization scheme. On the other hand, the latter method does not solve the evolution equations (2.14) literally, but only in the sense of a power expansion, i.e., up to terms of order $k \geq 2$. Therefore the first approach may be considered more in the spirit of the parton model, whereas the second is closer to a manifestly scheme independent expansion for physical observables.

### C. Small-$x$ resummed evolution

The resummed evolution of the parton distributions includes, to all orders in $a_s$, the most singular small-$x$ contributions to the splitting functions $P_k$. This inclusion is performed in the orders beyond the known fixed-order results. Thus the complete expressions for $P_0(N)$ and $P_1(N)$ are used also here, and the difference from the previous section is restricted to the higher-order matrices $P_{k \geq 2}$. Our notation in this section will directly apply to the evolution of unpolarized quark and gluon densities. Most of the subsequent discussion can, however, be easily transferred to the polarized singlet evolution [55] by replacing $1/N^{k+l}$ by $1/(N+1)^{2k+l}$ with correspondingly modified coefficient matrices in all expansions.

In the present case the most singular small-$x$ terms in the evolution equations (2.14) behave like $1/xa_s^{k+1}\ln^k x$ [4] and $1/xa_s^{k+1}\ln^{k-1} x$ [8] as discussed in Sec. III. In Mellin-$N$ space these additional resummation contributions replacing Eq. (5.15) read

$$P_{k \geq 2}^{\text{res}}(N) = \frac{P_k^{\text{L}x}}{N^{k+1}} + i_{\text{NL}} \frac{P_k^{\text{NL}x}}{N^k}. \quad (5.20)$$

In particular, the matrix $P_k^{\text{L}x}$ is related to the expansion coefficients $g_{k,gg}^{(0)}$ in Table I by

$$P_k^{\text{L}x} = (4C_A)^{k+1} g_{k,qq}^{(0)} \begin{pmatrix} 0 & 0 \\ C_F/C_A & 1 \end{pmatrix}. \quad (5.21)$$

$i_{\text{NL}}$ indicates whether only these leading small-$x$ pieces are taken into account (L$x$ resummation), or whether also the next terms in Eq. (5.20) are kept (NL$x$ resummation):

$$i_{\text{NL}} = \begin{cases} 0 & \text{for } Lx \text{ resummation}, \\ 1 & \text{for } NLx \text{ resummation}. \end{cases} \quad (5.22)$$

Recall that only the upper row of the NL$x$ matrix is completely known at present [8]. Results including that part only will be marked by NL$x_q$ below.

With respect to the solution of the evolution equations, the situation is analogous to the fixed-order case, with the expansion parameter $a_s$ replaced by $N$ at each order $k \geq 2$ of the strong coupling. The first option is obviously again the direct solution of Eq. (5.2), now after inserting Eqs. (5.16) and (5.20). To elucidate the generalization of the NLO$_{\text{tr}}$ procedure to the resummed evolution, consider the splitting functions contribution $R_{k \geq 2}$, Eq. (5.4), arising from Eq. (5.20):

$$R_{k \geq 2}^{\text{res}}(N)$$

$$= \frac{1}{N^{k+1}} \frac{1}{\beta_0} [P_k^{\text{L}x} + i_{\text{NL}} N P_k^{\text{NL}x}] - \frac{1}{N^k} \frac{\beta_1}{\beta_0^2} [P_{k-1}^{\text{L}x} + i_{\text{NL}} N P_{k-1}^{\text{NL}x}]$$

$$+ \frac{1}{N^{k-1}} \frac{1}{\beta_0} \left\{ \left(\frac{\beta_1}{\beta_0}\right)^2 - \frac{\beta_2}{\beta_0} \right\} [P_{k-2}^{\text{L}x} + i_{\text{NL}} N P_{k-2}^{\text{NL}x}] + \cdots.$$

$$(5.23)$$

The omitted terms involving higher powers of $\beta_1$ and $\beta_2$, or $\beta_{k \geq 3}$, are obviously even less singular as the last line for $N \to 0$. Therefore, if the power-counting in $N$ is done on the level of Eq. (5.2), one immediately arrives at

$$R_{k \geq 2}^{\text{res}'}(N) = \frac{1}{\beta_0} \frac{1}{N^{k+1}} \left[ P_k^{\text{L}x} + i_{\text{NL}} N \left( P_k^{\text{NL}x} - \frac{\beta_1}{\beta_0} P_{k-1}^{\text{L}x} \right) \right]. \quad (5.24)$$

Note that in the NL$x$ (L$x$) case the $\beta$-function coefficients $\beta_{k \geq 2}$ ($\beta_{k \geq 1}$) do not contribute any more, and that $\beta_1$ occurs only linearly in the former case. Thus $P_1$, which does not exhibit an L$x$ contribution, does not enter Eq. (5.24) in the present unpolarized case. All this is completely analogous to the $R$ matrices (5.18) for the NLO$_{\text{tr}}$ evolution.

Before we turn to the $U$ matrix for this second procedure, it is instructive to consider a small-$x$ approximation to the unpolarized L$x$ evolution in this approach. Unlike in any other QCD singlet case, including the polarized leading small-$x$ resummation [55], the splitting function combinations $R_{k,k' \geq 2}$ do commute here: $[R_k(N),R_{k'}(N)] = 0$, due to the simple structure of the matrix (5.21). This is still not sufficient for a closed solution of the evolution equation (5.2), unless one also keeps the leading small-$x$ contributions to $P_{0,1}(N)$ only. Then, however, one eigenvalue of $P_0$ vanishes, resulting in

$$P_0^{x \to 0} = \frac{4C_A}{N} \begin{pmatrix} 0 & 0 \\ C_F/C_A & 1 \end{pmatrix} = \frac{4C_A}{N} e_+^{x \to 0}. \quad (5.25)$$

Using Eqs. (3.4) one obtains with this additional approximation,

$$q_{Lx}^{\text{approx}}(a_s,N)=\exp\left[\frac{1}{2\beta_0}\int_{a_0}^{a_s}da\,\frac{1}{a^2}\boldsymbol{\gamma}_L(a,N)\right]\boldsymbol{q}(a_0,N)$$

$$=\exp\left(\frac{12L}{\beta_0 N}\right)\left[1+\sum_{l=1}^{\infty}\frac{d_l(a_s,a_0)}{N^l}\right]\boldsymbol{e}_+^{x\to 0}\boldsymbol{q}(a_0,N),$$

$$(5.26)$$

analogous to the complete resummed non-singlet solution; see Refs. [21]. This simple approximate expression, however, does of course not lead to any quark evolution. Equation (5.26) can be completely transformed to $x$-space (cf. Ref. [43]),

$$\boldsymbol{q}_{Lx}^{\text{approx}}(a_s,x)=F(a_s,a_0,x)\otimes\boldsymbol{e}_+^{x\to 0}\boldsymbol{q}(a_0,x), \quad (5.27)$$

with

$$F(a_s,a_0,x)=\frac{1}{x}\left[\delta(1-x)+\sqrt{\frac{12L}{\beta_0\log(1/x)}}I_1(z)\right.$$

$$\left.+\sum_{l=1}^{\infty}d_l(a_s,a_0)\left(\frac{\beta_0\log(1/x)}{12L}\right)^{(l-1)/2}I_{l-1}(z)\right],$$

$$(5.28)$$

where

$$z=2\left[\frac{12L}{\beta_0}\log\left(\frac{1}{x}\right)\right]^{1/2}, \quad L=\log\left(\frac{a_s}{a_0}\right), \quad (5.29)$$

and $I_\nu(z)$ denotes the Bessel functions of imaginary argument. Similar expressions, e.g. in the double-logarithmic approximations, were studied in detail long ago [65] and were also considered recently [66]. As compared to the complete $Lx$ solution, however, the approximation (5.27) yields gluon densities which are typically too large by a factor of 2 for an evolution from 4 to 100 GeV$^2$. Therefore we will not apply this approach in the following.

We now proceed with the general resummed solution corresponding to the truncated NLO treatment where $U_{k\geq 2}=0$; see Eq. (5.19). The generalization to the present case is to keep only those terms of $U_{k\geq 2}$ which arise from the $Lx$ and NL$x$ pieces of $\boldsymbol{R}_1$ and of $\boldsymbol{R}_{k\geq 2}$ in Eq. (5.23). Hence the NLO coefficient $\boldsymbol{U}_1'=\boldsymbol{U}_1$ is supplemented by

$$[\boldsymbol{U}_2',\boldsymbol{R}_0]=\boldsymbol{R}_2^{\text{res}'}+\boldsymbol{R}_1^S\boldsymbol{U}_1^S+2\boldsymbol{U}_2' \quad (5.30)$$

etc. Here $\boldsymbol{R}_1^S$ denotes the small-$x$ contribution of $\boldsymbol{R}_1$,

$$\boldsymbol{R}_1^S(N)=\frac{1}{\beta_0}\frac{1}{N^2}\left[\boldsymbol{P}_1^{Lx}+i_{NL}N\left(\boldsymbol{P}_1^{NLx}-\frac{\beta_1}{\beta_0}\boldsymbol{P}_0^{Lx}\right)\right],$$

$$(5.31)$$

and the corresponding expansion coefficient $\boldsymbol{U}_1^S$ is given by

$$[\boldsymbol{U}_1^S,\boldsymbol{R}_0]=\boldsymbol{R}_1^S+\boldsymbol{U}_1^S. \quad (5.32)$$

The final step analogous to the NLO$_{\text{tr}}$ method is to keep the non-(N)L$x$ parts of $\boldsymbol{U}_1$ only linearly also in the inverse matrix $\boldsymbol{U}^{-1}$ of Eq. (5.7). This leads to

$$\boldsymbol{U'}^{-1}(a,N)=\left[1+a\boldsymbol{U}_1^S(N)+\sum_{k=2}^{\infty}a^k\boldsymbol{U}_k'(N)\right]^{-1}$$

$$+a\{\boldsymbol{U}_1^S(N)-\boldsymbol{U}_1'(N)\}$$

$$\equiv\boldsymbol{U}_S^{-1}(a,N)-\{1-a\boldsymbol{U}_1^S(N)\}+1-a\boldsymbol{U}_1(N).$$

$$(5.33)$$

The last two terms represent the truncated NLO contribution. Insertion of this decomposition into Eq. (5.7) finally yields [with $\boldsymbol{L}\equiv\boldsymbol{L}(a_s,a_0,N)$ for brevity]

$$\boldsymbol{q}_{\text{tr}}^{\text{res}}(a_s,N)=[\boldsymbol{L}+a_s\boldsymbol{U}_1(N)\boldsymbol{L}-a_0\boldsymbol{L}\boldsymbol{U}_1(N)]\boldsymbol{q}(a_0,N)$$

$$+[\boldsymbol{U}_S(a_s,N)\boldsymbol{L}\boldsymbol{U}_S^{-1}(a_0,N)$$

$$-\boldsymbol{L}-a_s\boldsymbol{U}_1^S(N)\boldsymbol{L}+a_0\boldsymbol{L}\boldsymbol{U}_1^S(N)]\boldsymbol{q}(a_0,N).$$

$$(5.34)$$

The first line is the NLO$_{\text{tr}}$ result (5.19); the second line represents the resummation correction.

### D. Photonic solution

We now turn to the parton distributions of the photon. In terms of the running coupling, the corresponding inhomogeneous evolution equation (2.21) reads

$$\frac{\partial\boldsymbol{q}^\gamma(a_s,N)}{\partial a_s}=\frac{a_{\text{em}}\{\boldsymbol{k}_0(N)+a_s\boldsymbol{k}_1(N)+a_s^2\boldsymbol{k}_2(N)+\cdots\}}{-a_s^2\beta_0-a_s^3\beta_1-a_s^4\beta_2\cdots}+\text{had}$$

$$=-\frac{a_{\text{em}}}{a_s^2}\left[\boldsymbol{K}_0(N)+\sum_{l=1}^{\infty}a_s^l\boldsymbol{K}_l(N)\right]+\text{had}$$

$$\equiv\boldsymbol{K}(a_s,N)+\text{had}. \quad (5.35)$$

Here $a_{\text{em}}=\alpha/4\pi$ denotes the electromagnetic fine structure constant, and analogously to Eqs. (5.3) and (5.4) we have introduced

$$\boldsymbol{K}_0\equiv\frac{1}{\beta_0}\boldsymbol{k}_0, \quad (5.36)$$

$$\boldsymbol{K}_l\equiv\frac{1}{\beta_0}\boldsymbol{k}_l-\sum_{i=1}^{l}\frac{\beta_i}{\beta_0}\boldsymbol{K}_{l-i}. \quad (5.37)$$

Finally "had" stands for the RHS of the hadronic evolution equation (5.2), with $\boldsymbol{q}$ replaced by $\boldsymbol{q}^\gamma$. The homogeneous component, $\boldsymbol{q}_{\text{hom}}$, of the solution of Eq. (5.35) is as derived in Secs. V A–V C. Hence only the inhomogeneous part, $\boldsymbol{q}_{\text{inhom}}=\boldsymbol{q}^\gamma-\boldsymbol{q}_{\text{hom}}$ with $\boldsymbol{q}_{\text{inhom}}(a_0,N)=0$, needs to be discussed here. This solution can be represented in terms of the hadronic evolution operator (5.7) as

$q_{\text{inhom}}(a_s,N)$

$$= U(a_s,N)a_s^{-R_0(N)}\int_{a_0}^{a_s}da\,a^{R_0(N)}U^{-1}(a,N)K(a,N).$$

$$(5.38)$$

For the iterative solutions the remaining integral can be performed numerically. In the truncated procedures, on the other hand, $U^{-1}(a,N)$ has been expanded in Eqs. (5.19) and (5.33). In these cases the NLO photonic splitting functions, $k_1^i \equiv P_1^{i\gamma}$, should be treated in the same way as their hadronic counterparts $P_1^{ij}$ previously, reducing Eq. (5.37) to

$$K_1'=K_1=\frac{1}{\beta_0}\left(k_1-\frac{\beta_1}{\beta_0}k_0\right),\quad K_{l\geqslant2}'=0.\qquad(5.39)$$

In the following we will confine ourselves to physical factorization schemes like the $\text{DIS}_\gamma$ scheme [32] or the DIS scheme, where the photonic coefficient function $C_{2,\gamma}$ has been absorbed into the quark distributions. In these schemes $K(a_s,N)$ does not receive any $Lx$ and $NLx$ resummation corrections beyond the leading order, as discussed in Sec. III. Thus Eq. (5.39) applies to the $\text{NLO}_{\text{tr}}$ photon evolution as well as to the corresponding resummed case.

Inserting $U_{\text{NLO}'}^{-1}(a_s,N)=1-a_sU_1(N)$ and the expansion (5.39) into the inhomogeneous solution (5.38), the $a_s$ integration becomes obvious and one arrives at [32]

$$\frac{1}{a_{\text{em}}}q_{\text{inhom}}^{\text{NLO}'}(a_s,N)$$

$$=\frac{1}{a_s}[1+a_sU_1(N)]\left(1-\frac{a_s}{a_0}L\right)[1-R_0(N)]^{-1}K_0(N)$$

$$-(1-L)R_0^{-1}(N)[K_1(N)-U_1(N)K_0(N)]+O(a_s).$$

$$(5.40)$$

In the resummed case a numerical integration remains over the all-order part of $U'^{-1}$ in Eq. (5.33). Defining

$$\Delta_{\text{res}}(a_s,a_0,N)$$

$$=-\int_{a_0}^{a_s}\frac{da}{a^2}L^{-1}(a,a_0,N)[U_S^{-1}(a,N)-1+aU_1^S(N)]K_0(N)$$

$$(5.41)$$

the solution is, again using $L\equiv L(a_s,a_0,N)$, given by

$$\frac{1}{a_{\text{em}}}q_{\text{inhom}}^{\text{res}'}(a_s,N)=\frac{1}{a_e}q_{\text{inhom}}^{\text{NLO}'}(a_s,N)+U_s(a_s,N)\Delta_{\text{res}}(a_s,a_0,N)$$

$$+U_s(a_s,N)\left[\frac{1}{a_s}\left(1-\frac{a_s}{a_0}L\right)[1-R_0(N)]^{-1}K_0(N)+(1-L)R_0^{-1}(N)U_1^S(N)K_0(N)\right]$$

$$-[1+a_sU_1^S(N)]\frac{1}{a_s}\left(1-\frac{a_s}{a_0}L\right)[1-R_0(N)]^{-1}K_0(N)-(1-L)R_0^{-1}(N)U_1^S(N)K_0(N).\qquad(5.42)$$

This relation completes the Mellin-$N$ solutions of the fixed-order and resummed, hadronic and photonic evolution equations. We are now prepared to investigate the quantitative impact of the various approximations, for both the splitting functions and the solutions, on the parton densities and structure functions.

## VI. NUMERICAL RESULTS

In the following we study the numerical consequences of the fixed-order and resummed evolution kernels on the evolution of structure functions and some aspects related to potential uncertainties. Despite the impressive amount of small-$x$ structure function data already collected at HERA [1,2], the present investigation does not aim at a comparative data analysis. Such an effort would require quite some flexibility in the non-perturbative initial distributions, especially for the gluon density which is only rather indirectly constrained by measurements of $F_2$ and $F_L$. A detailed data analysis requires rather precise and independent constraints

on the small-$x$ behavior of the gluon density, which are not yet provided by current measurements at HERA. A thorough implementation of heavy flavor (charm) mass effects in the resummation framework would be required as well. These mass effects are non-negligible at small $x$, where the charm contribution to $F_2$ and $F_L$ is substantial, in spite of the very large hadronic invariant mass, $W^2\gg4m_c^2$; cf. Ref. [67]. Both of these issues lie beyond the scope of the present paper. Since some of the resummation corrections turn out to be very large, one would like to know as well the next-order resummed corrections to perform a detailed data analysis.

In the following, therefore, the impact of the various anomalous dimensions and Wilson coefficients is instead illustrated for fixed initial parton densities of the proton and the photon. Accordingly all calculations are performed using the same values for $\alpha_s(Q^2)$. Specifically, the NLO relation (2.10) is employed with $\Lambda_{N_f=4}=0.23$ GeV above $Q^2=m_c^2=(1.5\text{ GeV})^2$ and, by continuity of $\alpha_s(Q^2)$, with $\Lambda_{N_f=3}=0.30$ GeV below that scale. Above (below) $Q^2=m_c^2$ the evolution equations are solved for four (three) massless fla-
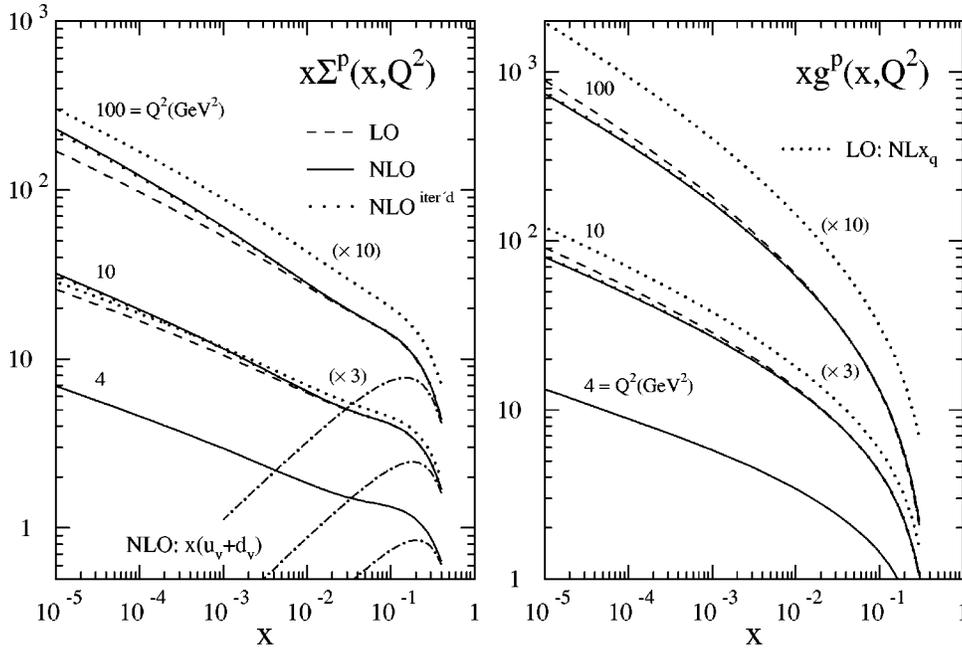
FIG. 5. The small-$x$ evolution of the proton's flavor-singlet quark and gluon distributions in LO and NLO perturbative QCD. Two approaches to the solution of the evolution equations are compared in the NLO case; cf. Sec. V. Also shown is the result of a small-$x$ approximation (NL$x_q$; see the text) of the LO splitting functions. The behavior of non-singlet quantities is illustrated by the total valence quark distribution $x(u_v + d_v)$.

vors, respectively, with $c(x, m_c^2) = \bar{c}(x, m_c^2) = 0$. The small effects of the bottom flavor are entirely neglected. All subsequent results are derived in the DIS scheme discussed above, with the truncated solutions of Sec. V chosen as default. Only the singlet resummations described in Sec. III are taken into account, since the non-singlet contributions are suppressed at small $x$ in the present unpolarized case (see Fig. 5), and its resummation correction is very small; cf. Sec. II B.

### A. Proton structure: Fixed-order evolution

Let us first consider the leading and next-to-leading order evolution of hadronic parton densities, putting emphasis on the small-$x$ region. As the value of $\Lambda_{N_f = 4}$ given above, the initial distributions for our proton studies are adopted from the Martin-Roberts-Stirling set A′ [MRS(A′)] global fit [62] at a reference scale $Q_0^2 = 4$ GeV$^2$. For the present purpose, the most relevant feature of these input densities is their small-$x$ behavior which has been constrained by previous HERA data:

$$xg^p(x, Q_0^2) \propto x\Sigma^p(x, Q_0^2) \propto x^{-0.17} \quad \text{for} \quad x \to 0. \quad (6.1)$$

Recall that, unlike the gluon distribution, the DIS-scheme quark densities represent observables.

The LO and NLO small-$x$ evolution of $x\Sigma^p$ and $xg^p$ to $Q^2 = 10$ and 100 GeV$^2$ is shown in Fig. 5 together with the initial distributions. The LO curves have been calculated, as indicated above, using the NLO input densities and $\alpha_s$ values in Eq. (5.6). Hence they do not represent results of an independent leading-order analysis, but directly illustrate the importance of the NLO terms relative to the LO contribution in Eq. (5.19). One notices that the perturbative stability of the presently available fixed-order evolution is theoretically satisfactory also at very low values of $x$. For instance, the NLO/LO ratio amounts to 1.25 (0.87) for the singlet (gluon)

density at $Q^2 = 100$ GeV$^2$ and $x = 10^{-4}$. Furthermore the numerical differences between the expanded solution (5.19) and the iterative approach (5.17) to the NLO evolution equations can be considered as absolute lower limits on the uncertainties due to the unknown higher-order splitting functions. These offsets reach 3% at $x \simeq 10^{-5}$, while amounting to less than 1% for $x \gtrsim 10^{-3}$; see also Fig. 6 below.[5] Thus one may roughly expect a 5–10 % small-$x$ effect from the 3-loop anomalous dimensions, if fixed-order renormalization group improved perturbation theory remains the appropriate framework down to $x \gtrsim 10^{-5}$. Such an estimate is also corroborated by studies of the factorization scale dependence of $F_2$ at small $x$ [20].

It is conceivable, however, that the NLO contributions to the small-$x$ anomalous dimensions are untypically small [as, for instance, $1/N^2$ terms are absent in $\gamma_1$; cf. Eqs. (4.2) and Table I]. In this context it is instructive to study the convergence of (formal) small-$x$ expansions of anomalous dimensions and Wilson coefficients into the series

$$\varphi(a_s, N) = \sum_{l=1}^{\infty} a_s^l \left[ \frac{\varphi_l^{\text{L}x}}{N^l} + \frac{\varphi_l^{\text{NL}x}}{N^{l-1}} + \frac{\varphi_l^{\text{NNL}x}}{N^{l-2}} + \cdots \right] \quad (6.2)$$

already at the LO and NLO level, where the full results are available. Also shown in Fig. 5, therefore, is the NL$x_q$ approximation to the leading-order evolution, for which just the $1/N$ terms of $\gamma_{gg}^{\text{LO}}$ and $\gamma_{gq}^{\text{LO}}$ are kept together with the leading $N \to 0$ constants in $\gamma_{qg}^{\text{LO}}$ and $\gamma_{qq}^{\text{LO}}$; see Eqs. (4.1). Note that this procedure is close to the well-known double-logarithmic

---

[5]In previous comparisons [20,68] deviations of up to 8% were found between these solutions. These large effects originated in the unfortunate choice of a traditional approximate NLO expression for $\alpha_s(Q^2)$, showing that the representation of the NLO solution of Eq. (2.8) tends to be relevant at the current accuracy of the data.
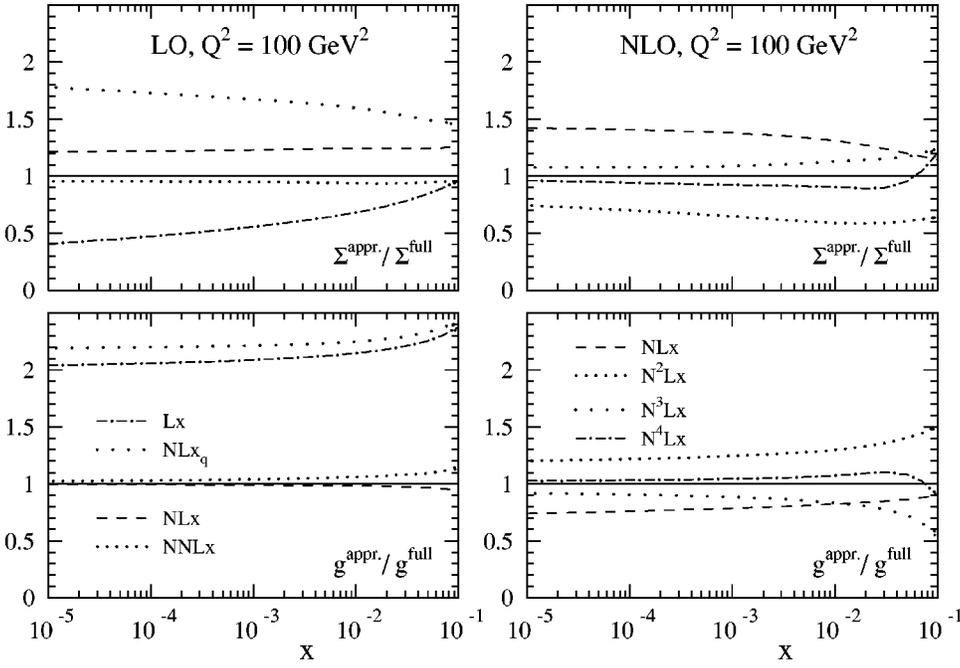
FIG. 6. The effects of the successive small-$x$ approximations (6.2) to the LO anomalous dimensions $\gamma_0$ (left) and to the NLO corrections $\gamma_1$ (right) on the low-$x$ evolution of $x\Sigma^p$ and $xg^p$; cf. Eqs. (4.1) and (4.2). All results are displayed at $Q^2 = 100$ GeV$^2$ relative to the respective full calculations presented in Fig. 5.

approximation; cf. Sec. V C. As can be seen from the figure, this first approximation is very poor: $x\Sigma$ and $xg$ exceed the full LO results by factors of about 1.7 and 2.2, respectively, rather uniformly in $x$ at $Q^2 = 100$ GeV$^2$, without any appreciable sign of improvement for decreasing values of $x$.

Hence the question arises as to how many terms in the small-$x$ expansion are required for arriving at a reasonably accurate representation of the complete fixed-order results. Accordingly, Fig. 6 displays the ratios $\Sigma^{\text{approx}}/\Sigma^{\text{full}}$ and $g^{\text{approx}}/g^{\text{full}}$ for the LO and NLO evolutions with an increasing number of terms taken into account in the expansion (6.2) of $\gamma_0$ and $\gamma_1$ (in NLO the complete expression for $\gamma_0$ has been employed for all curves). One finds that in general three to four non-trivial small-$x$ terms, i.e., contributions up to N$^2$L$x$ at LO and N$^3$L$x$ at NLO, are needed to achieve an accuracy of better than 10%. The NLO situation is not a peculiarity of the DIS scheme chosen here, as a corresponding $\overline{\text{MS}}$ analysis using Eqs. (4.3) yields similar results. Note that an interesting pattern emerges in both fixed-order cases: the approximate results alternate around the exact values with decreasing amplitude. If such a pattern were to persist to higher orders in $\alpha_s$, a first reliable estimate of their possible impact could be derived once two more non-trivial terms in all small-$x$ expansions were known. This aspect may be of relevance for the resummed evolution addressed in the following.

### B. Resummed evolution

We now turn to the effects and the relative importance of the L$x$ [4] and NL$x$ [8–10] higher-order contributions to the splitting functions discussed in Sec. III. In the present subsection the momentum sum rule (2.17) is restored by prescription (A) of Eq. (4.4); i.e., $P_k^{gg}$ and $P_k^{qq}$ are supplemented by appropriate $\delta(1-x)$ terms at all orders $k \geq 2$. This procedure is the one with the least impact on the small-$x$ results.

Without any subtraction the sum rule would be violated by about 1% and 6% at $Q^2 = 100$ GeV$^2$ for the L$x$ and NL$x_q$ resummed evolutions, respectively, of our MRS(A$'$) initial distributions.

The resulting evolutions of the singlet quark and gluon densities are compared to the NLO distributions in Fig. 7 for $Q^2 = 10$ and 100 GeV$^2$. The relative importance of the available gluonic (lower row) anomalous dimensions is illustrated in Fig. 8(a). Consider first the effect of the L$x$ corrections [4]. These terms exert an appreciable influence on the gluon evolution, but much less on the quark densities in the kinematic region covered by the figure. At $x = 10^{-4}$ and $Q^2 = 100$ GeV$^2$, e.g., ratios of $g^{Lx}/g^{NLO} = 1.24$ and $\Sigma^{Lx}/\Sigma^{NLO} = 1.07$ are obtained. This pattern obviously arises from the matrix structure of the L$x$ kernel (3.4); only at higher scales does the quark effect fully approach the gluon enhancement.

The inclusion of the NL$x_q$ terms [8], i.e. the upper row entries in Eq. (3.11), leads to only a small additional effect on $xg(x,Q^2)$. The impact of these terms on $x\Sigma(x,Q^2)$ is, however, exceedingly large, as already evident from Fig. 2. These effects have been illustrated before, cf. Refs. [44,23], partly using different parametrizations for the input distributions at the starting scale $Q_0^2$. The resulting enhancement with respect to the NLO evolution amounts to a factor of 2.8, for example, at $x = 10^{-4}$ and $Q^2 = 100$ GeV$^2$. This huge correction is indeed entirely driven by the quarkonic anomalous dimensions, as also illustrated in Fig. 8(a): any "reasonable" change of the gluonic splitting functions affects $x\Sigma$ by at most about 10%. Since only this one resummation contribution is known for the dominant upper-row quantities, a theory based estimate along the lines of Sec. VI A is not yet possible for the resummed quark distributions, and hence for the most important structure function, $F_2$. We will therefore resort to the sum-rule prescriptions of Sec. IV in the next subsection.
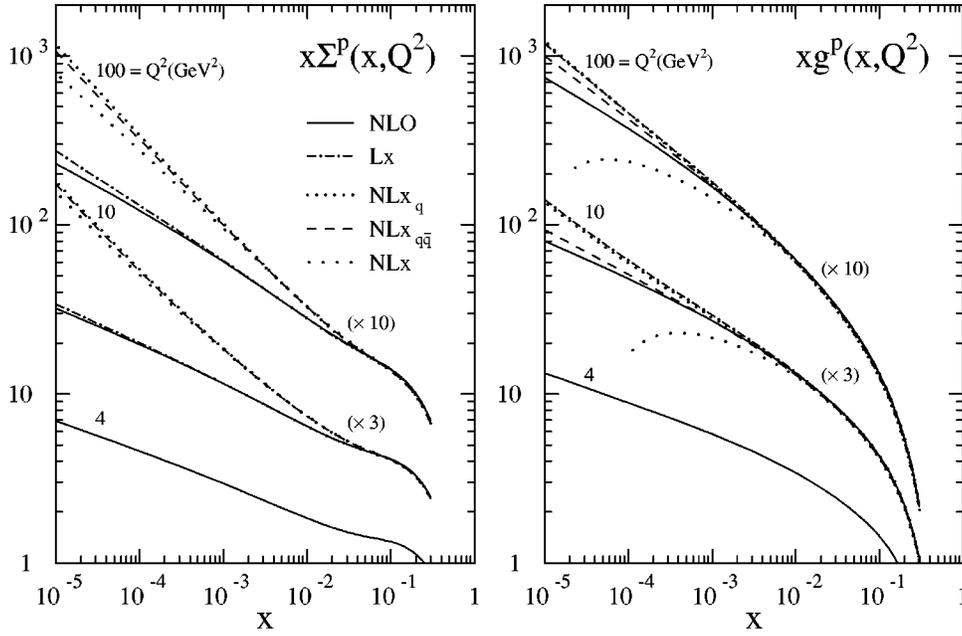
FIG. 7. The resummed small-$x$ evolution of the singlet quark and gluon densities as compared to the NLO results. The L$x$ [4] and NL$x$ [8–10] contributions are successively included, with the momentum sum rule implemented via prescription (A) of Sec. IV. The results for $Q^2 = 10$ and 100 GeV$^2$ have been multiplied by the factors indicated in the plots.

In the gluonic sector, on the other hand, the theoretical situation has been improved recently by Refs. [9,10]; see Sec. III. We remind the reader that the latter findings for $\gamma_{gg}$, although indicative, are not final yet, since the so-called energy-scale dependent NL$x$ terms have still to be calculated. The effects of the known next-to-leading contributions are also presented in Figs. 7 and 8(a). The well-established $q\bar{q}$ contribution to $\gamma_{gg}^{(1)}$ [9], which is not expected to yield the largest subdominant terms, already removes more than half of the L$x$ effects on the gluon density at $x \lesssim 10^{-4}$ for $Q^2 = 100$ GeV$^2$; see Fig. 8(a). The energy-scale independent gluonic contribution [10] overcompensates the enhancement

by the L$x$ and NL$x_q$ terms at all $x$ in Fig. 7. As expected from Fig. 3, these terms are so large that they even cause a sign change in the slope of the gluon evolution for $x \lesssim 10^{-4}$. It seems natural to expect that yet missing terms either in NL$x$ or unknown terms emerging in higher orders correct this behavior again. Thus a first uncertainty band of the possible resummation effects on $xg(x,Q^2)$ seems close to completion. In this context it should be recalled that the NL$x$ anomalous dimension matrix is not yet complete, as $\gamma_{gq}^{(1)}$ still remains uncalculated. Note, however, that $\gamma_{gq}^{(0)}$ has an impact of less than 10% on both $x\Sigma$ and $xg$ in the L$x$ and NL$x_q$ evolutions; cf. Fig. 8(a). Hence $\gamma_{gq}^{(1)}$ is presumably not
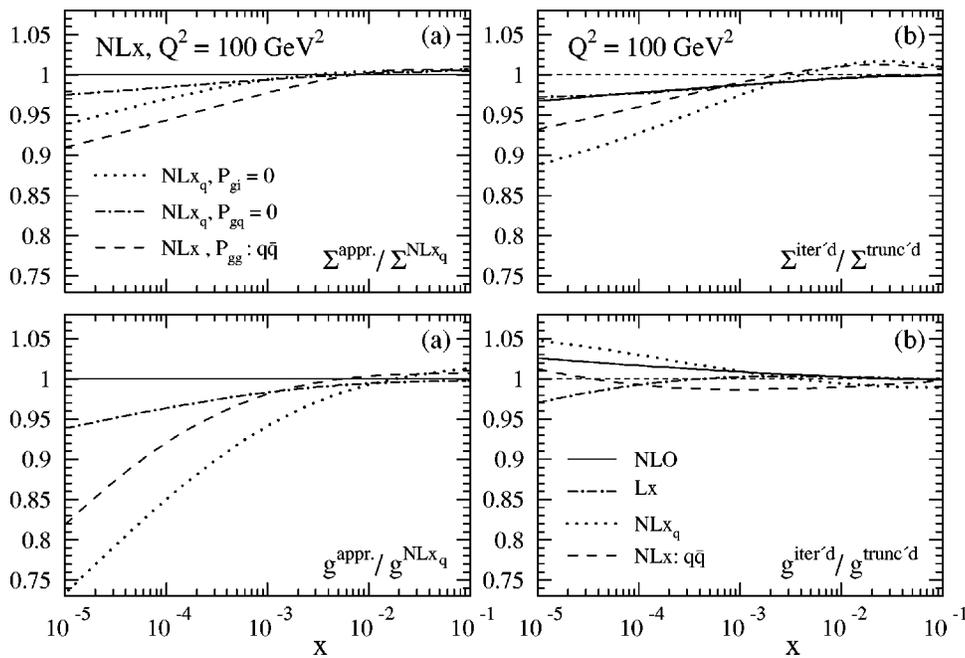


FIG. 8. (a) The impact of the resummed gluonic splitting functions $P_{gg}$ and $P_{gq}$ of Refs. [4,8,9] on $x\Sigma^p$ and $xg^p$ at $Q^2 = 100$ GeV$^2$. The NL$x_q$ results of Fig. 7 have been chosen as reference. (b) The offsets between the iterated and the truncated solutions of the evolution equations (see Sec. V) for the NLO case and various resummation approximations. In all other figures the truncated solutions have been employed.
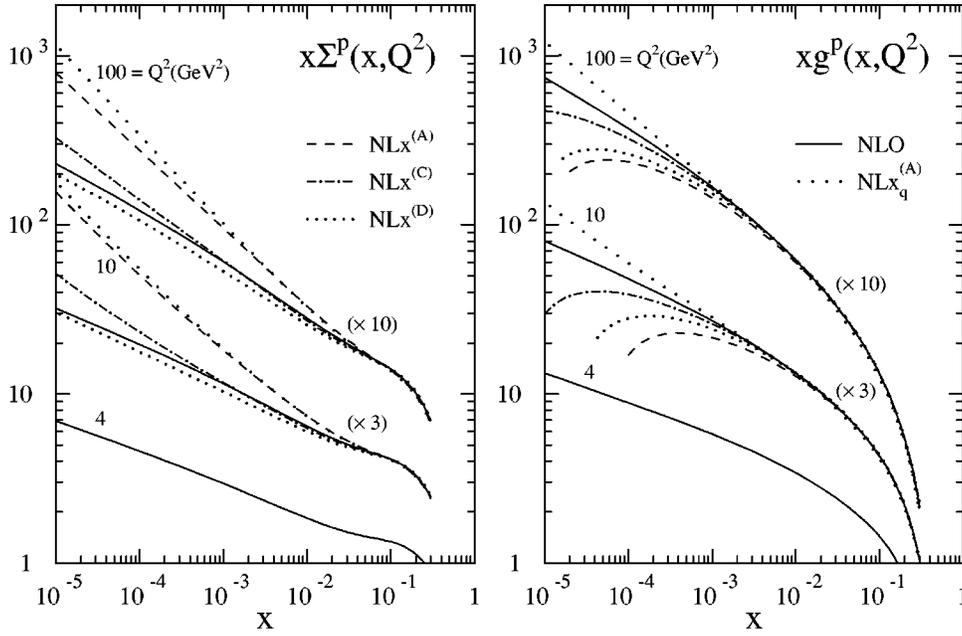
FIG. 9. The possible effects of subleading corrections to the resummed anomalous dimensions, exemplified by the momentum sum-rule prescriptions (C) and (D) of Eq. (6.3), on the small-$x$ evolution of the proton's parton densities. The results using the $\delta(1-x)$ subtractions (A) are as in Fig. 7. The MRS(A$'$) [62] initial distributions (transformed to the DIS scheme) have been employed as in all other proton figures.

a major source of uncertainty, as one may expect a rather moderate effect of this quantity as well.[6]

As in the NLO case of Sec. VI A, the differences between the iterative and the truncated solutions, Eqs. (5.23) and (5.34), of the evolution equations should yield a lower limit on the uncertainty due to missing terms in the anomalous dimensions. In fact, if the present small-$x$ resummations collected the most relevant higher-order terms, a reduction of these offsets should take place with respect to the NLO evolution. The corresponding results are depicted in Fig. 8(b). While staying on the same level as in the NLO case for the L$x$ evolution, the offsets increase significantly as soon as the NL$x$ terms are included, in particular for the singlet quark density: ratios $\Sigma^{\text{iter}'d}/\Sigma^{\text{trunc}'d}$ of up to about 10% are found. This decreased stability may point to a larger uncertainty of the huge NL$x$ quark enhancement.

### C. Structure functions and less singular terms

Less singular (subleading) contributions to the anomalous dimensions, i.e., terms which do not exhibit the leading $N \to 0$ behavior, are vitally important for the LO and NLO evolution at small $x$, as demonstrated in Fig. 6: three to four terms in the expansion (6.2) are required for a good representation. In higher orders of $\alpha_s$ the leading $N \to 0$ poles become more singular, but so do the subleading contributions, and the number of singular pieces increases. There is, therefore, no obvious reason to expect terms less singular in $N$ to be unimportant at low $x$ in all-order approaches. At the present stage of theoretical development, however, one has to rely on reasonable estimates for obtaining a first impression of their possible impact. For this purpose, we employ

the momentum sum-rule prescriptions (C) and (D) of Eq. (4.4) for all anomalous dimensions with only one all-order term known presently,

$$\gamma_{k \geqslant 2}^{ij}(N) \to \gamma_{k \geqslant 2}^{ij}(N)(1 - 2N + N^{\alpha}) \quad \text{for} \quad ij = qq, qg, gq.$$
(6.3)

Here $\alpha = 2$ [3] for the prescriptions (C) [(D)]. In $\gamma_{gg}$ we adopt the presently known NL$x$ contributions, which are taken from Table I. Hence only the $N^2$ or $N^3$ terms in this quantity are adjusted according to Eq. (2.17). In view of the structure of the $N$-expansions of the LO and NLO terms estimates like Eq. (6.3) are conservative; i.e., they might underestimate the present uncertainties.

In Fig. 9 the resulting singlet quark and gluon densities are compared at NL$x$ accuracy to distributions evolved with prescription (A). The subleading terms of the *Ansatz* (D) are sufficient to overcompensate the huge leading resummation effect on $x\Sigma(x,Q^2)$ slightly. E.g., the NL$x^{(D)}$ result falls about 10% short of the NLO distribution at $x = 10^{-4}$ and $Q^2 = 100$ GeV$^2$. Note that even the difference between prescriptions (C) and (D), arising from the replacement of parametrically small N$^3$L$x$ by N$^4$L$x$ terms in the quarkonic anomalous dimensions, proves rather appreciable. This situation is similar for $xg(xQ^2)$, where the effects of the sum-rule induced terms are positive because of the very large negative $\gamma_{gg}^{(1)}$ entries; cf. Table I. The order of the curves is different here as compared to $x\Sigma$, since $\gamma_{gg}$ differs between cases (A), (C), and (D) only in the third term of the small-$x$ expansion, unlike $\gamma_{qg}$ which dominates the quark evolution. Although definite conclusions cannot be drawn from these prescription-dependent results, they nevertheless indicate clearly that the $1/N$ expansion (6.2) behaves similar as in the fixed-order cases.

We now turn to the proton structure functions $F_2$ and $F_L$. Their small-$x$ behavior, as obtained from the parton densities just discussed, is displayed in Fig. 10. Since our calculations

_____

[6]This expectation is also supported by the fact that $\gamma_{gq}^{(1)}$ does not contribute to the eigenvalues of the resummed anomalous dimension matrix up to the NL$x$ level; see Eq. (3.15).
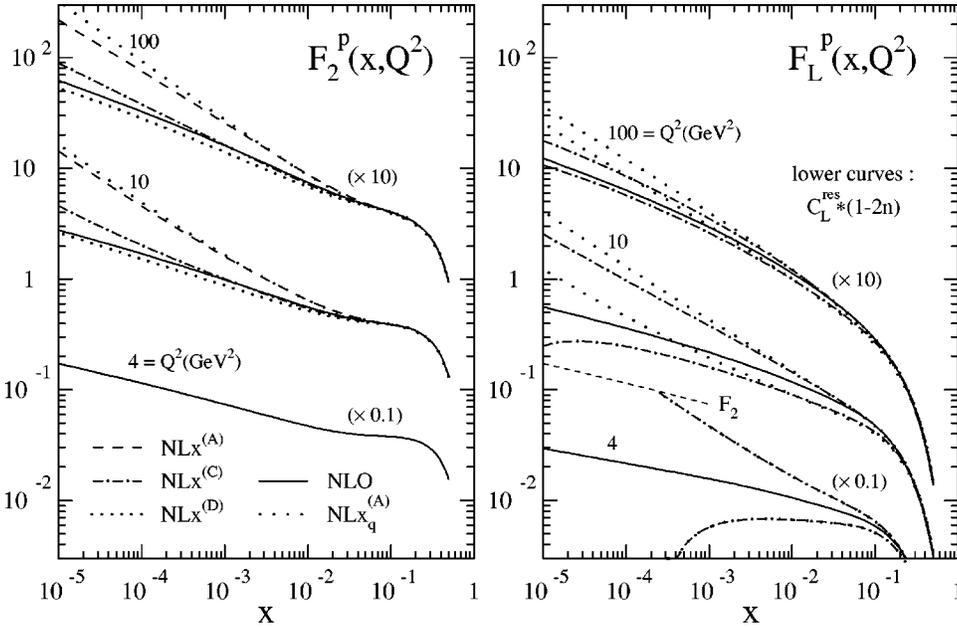
FIG. 10. The small-$x$ behavior of the resummed structure functions $F_2$ and $F_L$ for the parton evolutions shown in the previous figure in comparison with the NLO results. The upper $F_L$ curves include the resummed coefficient functions $C_L$ [8] [cf. Eq. (6.4)]; the lower ones illustrate the possible impact of a subleading contribution to $C_L$.

are performed in the DIS scheme, $F_2$ is very closely related to the quark singlet distribution at small $x$. Thus the left side of Fig. 10 exhibits a pattern very similar to Fig. 9. The longitudinal structure function, on the other hand, in addition involves the resummed coefficient functions

$$C_L(\alpha_s,N)=a_s C_{L,0}(N)+a_s^2 C_{L,1}(N)+\frac{4}{3}N_f a_s \sum_{k=2}^{\infty} c_k^L \left(\frac{\bar{\alpha}_s}{N}\right)^k.$$

$$(6.4)$$

$C_{L,0}$ and $C_{L,1}$ represent the leading and next-to-leading order [69,37] coefficient functions, and the gluon and pure singlet resummation coefficients [8] $c_k^L$ are given in Table I and Eq. (3.25).

The additional corrections due to the coefficients $c_k^L$ are, in fact, very large at the lower $Q^2$ values shown: even the cross-section positivity constraint $F_L<F_2$ is violated for $x \lesssim 3\times10^{-4}$ at $Q^2\simeq4$ GeV$^2$ for the Martin-Roberts-Stirling set A$'$ [MRS(A$'$)] initial distributions. At high $Q^2 \gtrsim100$ GeV$^2$ the effects of the coefficient functions and of the parton evolution become comparable due to the decrease of $\alpha_s$ in $C_L(\alpha_s,N)$. The size of the low-$Q^2$ effect shown in Fig. 10 (upper dotted and dash-dotted curves), however, requires sizable corrections by yet unknown higher-order terms in the small-$x$ resummation of $C_L$ or a large adjustment of the input gluon density. In fact, also the coefficient functions can be expected to receive relevant subleading corrections which are unknown at present. In order to derive a first estimate on their possible impact, the $F_L$ calculations have been repeated with

$$c_{k\geqslant2}^L \to c_{k\geqslant2}^L (1-2N).$$

$$(6.5)$$

The results of these calculations are shown in Fig. 10 (lower curves). This moderate correction term leads to an even drastic overcompensation of the leading resummation effect at low $Q^2$. This shows that for a more detailed understanding of

the small-$x$ behavior of $F_L(x,Q^2)$ the next-order small-$x$ resummed corrections are required. On the other hand, direct measurements of $F_L(x,Q^2)$ by the HERA experiments[7] could help to constrain the size of missing terms in the coefficient functions.

### D. Photon structure at small $x$

We now address, finally, the small-$x$ evolution of the parton densities of the real photon. As outlined in Sec. II, this evolution includes a specific inhomogeneous (''pointlike'') piece in addition to the homogeneous (''hadronic'') component. Whereas the latter behaves rather similar to the proton's parton distribution considered in the preceding subsections, the former is completely calculable in perturbation theory up to its dependence on the starting scale $Q_0^2$. As discussed in Sec. III one may study the evolution of the photon structure function in a DIS scheme, where the inhomogeneous part does not involve any new resummed splitting functions at the present level of accuracy. It does, however, probe the resummed hadronic evolution matrix in a specific, different manner (cf. Sec. V), and thus provides an additional laboratory for studying the possible effects of the small-$x$ resummations.

The reference scale $Q_0^2$ takes a somewhat different character in the photon case than in the pure hadronic evolution. It is a free parameter for the solution of the evolution equations, still, but only for certain choices of $Q_0^2$ can the separation between the homogeneous and inhomogeneous pieces approximately reflect the physical decomposition into the non-perturbative component, induced, e.g., by vector meson

---
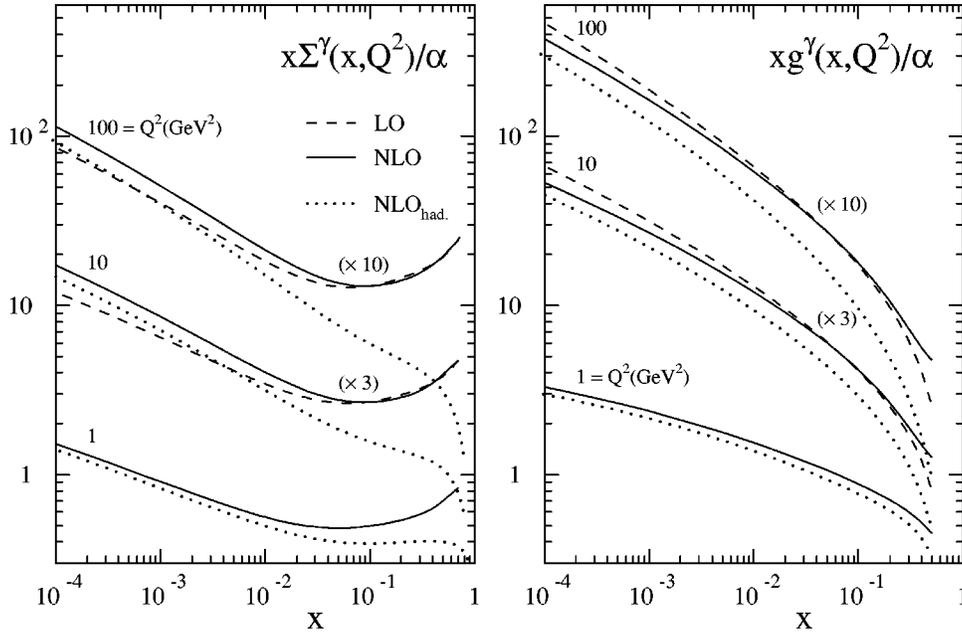
FIG. 11. The small-$x$ evolution of the photon's singlet quark and gluon distributions in leading and next-to-leading order, starting from the NLO parametrization of [70] at $Q_0^2 = 1$ GeV$^2$ as in all following figures. The hadronic (vector-meson-dominance induced) components are compared to the full results at NLO.

dominance (VMD) and a perturbative contribution. In fact this physical decomposition leads to $Q_0^2 < 1$ GeV$^2$ [70,71]; for a recent overview cf. Ref. [72]. We therefore choose $Q_0^2 = 1$ GeV$^2$ in the following, unlike the proton case of Sec. VI A–VI C. At this scale we adopt the NLO photonic parton distributions of Glück, Reya and Vogt (GRV) [70], as this is the only available NLO set with a HERA-like small-$x$ rise of the hadronic component. The low-$x$ behavior of these singlet and gluon densities is not given by a simple power law (6.1), however, but can approximately be written as

$$\Sigma^\gamma(x, Q_0^2) \sim x^{-0.22}, \quad g^\gamma(x, Q_0^2) \sim x^{-0.13 \cdots -0.22}$$

$$\text{for } 10^{-4} \lesssim x < 10^{-2}. \tag{6.6}$$

Here the effective rising power of $xg^\gamma$ decreases with decreasing $x$; cf. Ref. [64].

The fixed-order evolution of $x\Sigma^\gamma$ and $xg^\gamma$ is recalled in Fig. 11. As in the proton case, the LO solution has been calculated using the NLO (DIS scheme) initial distributions and the NLO values for $\alpha_s(Q^2)$. The NLO-LO difference is slightly larger than in Fig. 5 due to the larger values of the coupling constant involved. Also shown in the figure is the NLO hadronic VMD contribution which is suppressed (in particular in the quark case) at large $x$, but dominant in the small-$x$ regime: it still amounts to about 80% of the full results for $x < 10^{-3}$ at $Q^2 = 100$ GeV$^2$. Therefore one may expect a similar rise of $F_2^\gamma$ as observed for $F_2^p$ at HERA [1]. We shall consider now how the resummation corrections affect this picture.

Figure 12 presents the effects of the various resummed small-$x$ terms [4,8–10] on the evolution of the singlet quark and gluon distributions. The full results and the inhomogeneous contributions for $Q_0^2 = 1$ GeV$^2$ are separately shown. These effects are considerably larger than those in Fig. 7: the NL$x$/NLO ratios reach factors of about 8 and 2 here for $x\Sigma^\gamma$ and $xg^\gamma$, respectively, at $x = 10^{-4}$ and $Q^2 = 100$ GeV$^2$. The

dominant sources of this greater enhancement are again the larger $\alpha_s$ values implied by the lower choice of $Q_0^2$. The inhomogeneous components are still suppressed, although they are even more affected by the resummation corrections, as factors of up to 15 and 8 are found for the NL$x$/NLO ratios of $\Sigma_{\text{inhom}}$ and $g_{\text{inhom}}$, respectively.[8] Recall that these latter results do not depend on any non-perturbative input distributions. Note also that $xg_{\text{inhom}}$ is much less affected by the $\gamma_{gg}^{(1)}$ corrections [9,10], since the main "driving term" of the inhomogeneous solution is the purely quarkonic quantity $k_0$; cf. Eq. (5.42).

The possible effects of less singular terms, using the same momentum sum-rule prescription as in the proton evolution, are illustrated in Fig. 13 for $F_2^\gamma$ and $xg^\gamma$. The general pattern for the total results is analogous to the purely hadronic case of Figs. 9 and 10. The relevance of subleading corrections, however, is even more enhanced than that of the leading terms: $F_2^\gamma$ falls far below the NLO calculation for the *Ansatz* (D), and the breakdown of the gluon evolution in NL$x^{(A)}$ already takes place at $x \lesssim 10^{-3}$. On the other hand, the less singular terms are much less effective in $F_{2,\text{inhom}}$ at small $x$. In hadron-like cases their importance is magnified by the convolution with the (soft) parton densities; cf. Figs. 2 and 3. Here, however, the function $xk_0^q \propto x[1 + (1-x)^2]$, which plays the role of an "input distribution," is very hard. Hence $F_{2,\text{inhom}}$ comes closer to a local probe of the small-$x$ splitting functions than any inclusive hadronic quantity.

Nevertheless, the inhomogeneous part remains much smaller than that homogeneous piece of $F_2^\gamma$ for most scenarios of Fig. 13. It should be noted, however, that the latter contribution may be suppressed down to about the NLO results by a different choice of $xg^\gamma$. It is conceivable, there-

---

[8]In contrast, the NLO/LO ratio not shown in the figure is on a rather normal level.
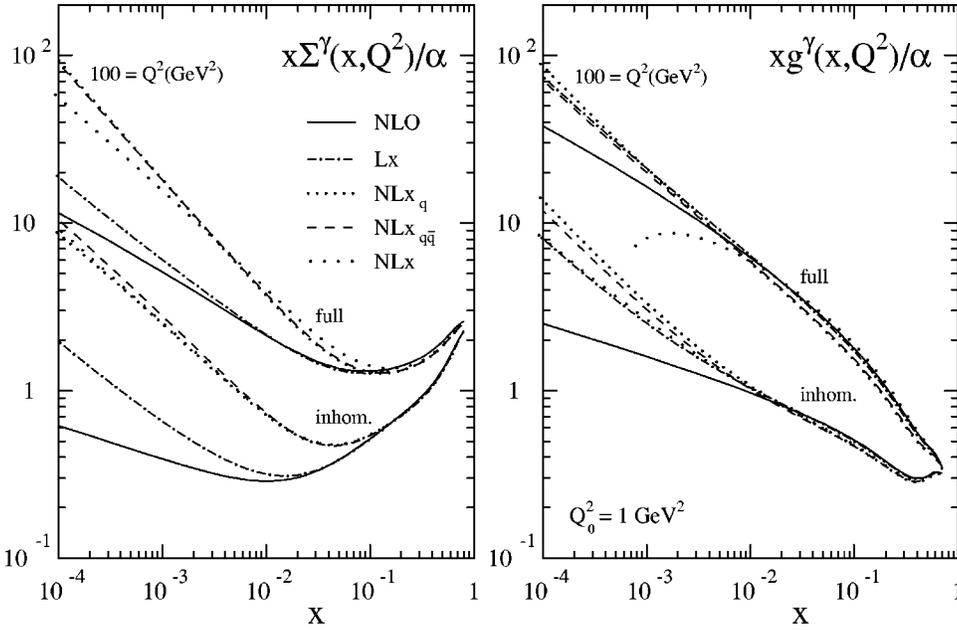
FIG. 12. The resummed small-$x$ evolution of $x\Sigma^{\gamma}$ and $xg^{\gamma}$ to $Q^2 = 100$ GeV$^2$ as compared to the NLO results. The L$x$ [4] and NL$x$ [8–10] contributions are successively included, with the momentum sum rule implemented via prescription (A) of Sec. IV. The effects on the photon-specific inhomogeneous solution are displayed separately.

fore, that $F_{2,\text{inhom}}$ is much more important in the resummed evolution than in the fixed-order case discussed above. Indeed, a small-$x$ $F_2^{\gamma}$ considerably greater than about 1.2 times the VMD expectation could be considered as a signal for the presence of large resummation corrections in the quarkonic anomalous dimension. A measurement of $F_2^{\gamma}$ in the small-$x$ region will, however, presumably only be possible with the $e\gamma$ mode of a future $e^+e^-$ linear collider.[9] Another theoretically cleaner, but experimentally also very difficult probe would be the structure of highly virtual photons, where the non-perturbative VMD part is suppressed and the calculable part becomes more important; cf. Ref. [74].

## VII. CONCLUSIONS

The effects of the resummation of the L$x$ and the known NL$x$ small-$x$ contributions to the flavor-singlet anomalous dimensions and coefficient functions have been investigated, in a framework based on the renormalization group equations, for the DIS structure functions $F_2^p$ and $F_L^p$ as well as for the photon structure function $F_2^{\gamma}$. In this approach direct comparisons are possible with studies of the scaling violations of these structure functions based on LO and NLO fixed-order calculations. In order to allow for the most flexible comparison of different approximations to the all-order
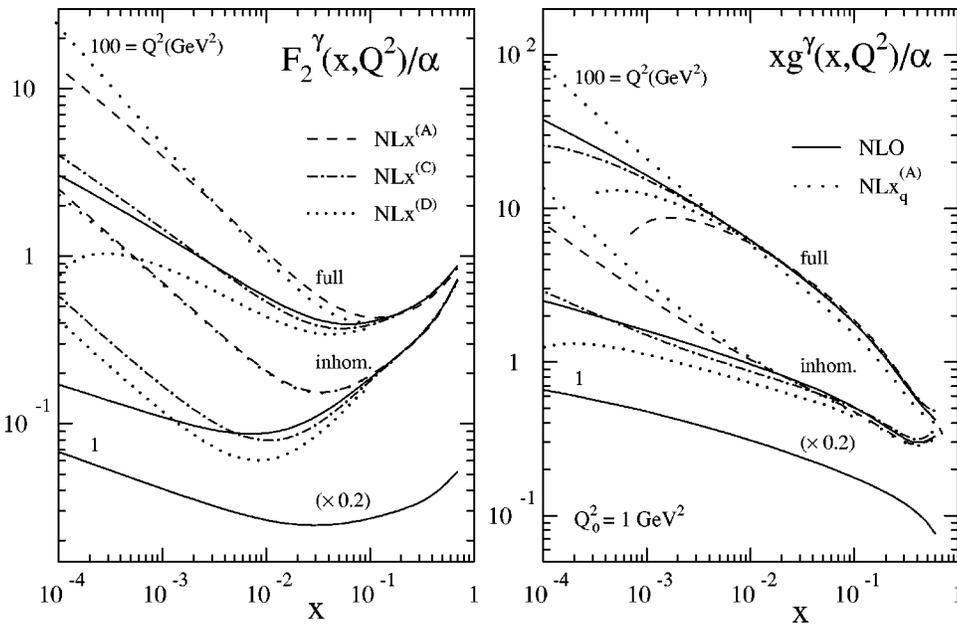


FIG. 13. The possible effects of subleading corrections to the resummed evolution kernels, exemplified by the momentum sum-rule prescriptions (C) and (D) of Eq. (6.3), on the small-$x$ evolution of the photon structure function $F_2^{\gamma}$ and the photon's gluon distribution.

---

[9]The possible kinematic coverage and necessary detector requirements have been studied in Ref. [73].

evolution equations, their general analytic moment-space solution has been derived.

The largest small-$x$ corrections to the quark densities and $F_2$ are due to the resummed quarkonic NL$x$-corrections [8], whereas the effect of the gluonic terms is marginal here. For the gluon density, the L$x$ corrections [4] are moderately positive. Both the quarkonic [9] and the energy-scale independent gluonic [10] parts of the NL$x$ gluon-gluon anomalous dimension, on the other hand, cause negative corrections which are so large that they overcompensate the L$x$-terms. In fact, the latter terms lead to negative values for the total splitting function $xP_{gg}(x, \alpha_s)$ for $\alpha_s = 0.2$ and $x < 10^{-2}$. This behavior probably signals the presence of other large positive contributions, either due to the energy-scale dependent NL$x$-terms or originating in terms of NNL$x$ or even higher order.

Contributions of NNL$x$ order exhibiting a similar behavior can as well exist in the case of the quarkonic anomalous dimensions and the coefficient functions. This is suggested, for example, by the expansion of the fixed-order anomalous dimensions in powers of $1/N$ which leads to a good approximation only after three to four terms. Different *Ansätze* for potential less singular terms have been studied numerically, showing that even the exceedingly large corrections due to the quarkonic NL$x$-corrections can easily be removed again.

The longitudinal structure function $F_L$ is in addition affected by the small-$x$ contributions to the coefficient functions $C_L$ [8]. For lower values of $Q^2$ the corrections become so large that the positivity constraint $F_L < F_2$ can be violated for conventional input parton distributions. However, also this resummed coefficient function is very sensitive to subleading corrections.

All these aspects show that also the next less singular terms need to be calculated, despite the enormous work that has been carried out so far to derive the resummed anomalous dimensions and coefficient functions [4,8–10,48,49], before firm conclusions on the small-$x$ evolution of singlet structure functions can be drawn. Since contributions which are even less singular than these ones may even then cause relevant corrections, it appears indispensable to compare the

corresponding results to those of future complete fixed-order calculations. There the medium and large $x$ terms are fully contained up to the respective order in $\alpha_s$. If extended to higher orders, in fact, also the RGE-improved fixed-order perturbation theory still seems to remain a viable candidate for the theoretical framework in the HERA regime.

The small-$x$ evolution of the real photon's parton structure has been analyzed in the DIS scheme. It has been shown that this scheme can be defined, without loss of generality, in such a manner that the photon-parton splitting functions do not receive any higher-order resummation corrections at NL$x$ accuracy. Nevertheless, the photon structure function $F_2^\gamma$ can provide an additional laboratory for studying the possible effect of small-$x$ resummations, as the characteristic, calculable inhomogeneous solution of the evolution equations probes the low-$x$ hadronic anomalous dimensions in a unique way: it comes closer to a local probe of the small-$x$ quarkonic splitting functions than any inclusive hadronic quantity. Unfortunately, this particularly interesting contribution is likely to be dominated by the hadron-like vector-meson-dominance part which behaves completely analogous to the photon structure and hence introduces the same uncertainties and limitations due to the interplay of the anomalous dimensions and the non-perturbative initial distributions.

*Note added in proof.* After the completion of this paper, a first calculation has been performed from which the complete NL$x$ gluon-gluon anomalous dimension can be inferred; cf. our discussion in Sec. III B. While this new result has some quantitative impact ($xP_{gg}$ turns negative even at a somewhat larger $x$ than in Fig. 3), our respective conclusions remain unchanged. For further details, the reader is referred to [75].

[1] H1 Collaboration, C. Adloff *et al.*, Nucl. Phys. **B497**, 3 (1997); H1 Collaboration, S. Aid *et al.*, *ibid.* **B470**, 3 (1996); ZEUS Collaboration, M. Derrick *et al.*, Z. Phys. C **69**, 607 (1996); **72**, 399 (1996); ZEUS Collaboration, J. Breitweg *et al.*, Phys. Lett. B **407**, 432 (1997); V. Chekelian, in Proceedings of the XVIII International Symposium on Lepton-Photon Interactions, Hamburg, 1997; R. Devenish, in Proceedings of the European Conference on High Energy Physics, Jerusalem, 1997.

[2] H1 Collaboration, C. Adloff *et al.*, Phys. Lett. B **393**, 452 (1997); H1 Collaboration, in Proceedings of the European Conference on High Energy Physics, Jerusalem, 1997.

[3] K. G. Wilson, Phys. Rev. **179**, 1699 (1969); R. A. Brandt and G. Preparata, Fortschr. Phys. **18**, 249 (1970); W. Zimmer-

mann, in *Elementary Particle Physics and Quantum Field Theory*, Proceedings of the 1970 Brandeis Summer Institute, edited by S. Deser, M. Grisaru, and H. Pendleton (MIT Press, Cambridge, MA, 1974), Vol. 1, p. 396; Y. Frishman, Ann. Phys. (N.Y.) **66**, 373 (1971); N. Christ, B. Hasslacher, and A. H. Mueller, Phys. Rev. D **6**, 3543 (1972); S. A. Anikin and O. I. Zavialov, Ann. Phys. (N.Y.) **116**, 135 (1978); O. I. Zavialov, *Renormalized Quantum Field Theory* (Kluwer Academic, Dordrecht, 1990).

[4] L. N. Lipatov, Sov. J. Nucl. Phys. **23**, 338 (1976); E. A. Kuraev, L. N. Lipatov, and V. S. Fadin, Sov. Phys. JETP **45**, 199 (1977); Phys. Lett. **60B**, 50 (1975); B. M. McCoy and T. T. Wu, Phys. Rev. Lett. **35**, 604 (1975); A. L. Mason, Nucl. Phys. **B117**, 493 (1976); **B120**, 275 (1977); C. Y. Lo and H.

Cheng, Phys. Rev. D **15**, 2959 (1977); I. I. Balitskii and L. N. Lipatov, Sov. J. Nucl. Phys. **28**, 822 (1978); J. Bronzan and R. Sugar, Phys. Rev. D **17**, 585 (1978); T. Jaroszewicz, Acta Phys. Pol. B **11**, 965 (1980); Phys. Lett. **116B**, 291 (1982); L. N. Lipatov, Sov. Phys. JETP **63**, 904 (1986); M. Ciafaloni, Nucl. Phys. **B296**, 49 (1988); for reviews see H. Cheng and T.T. Wu, *Expanding Protons: Scattering at High Energies* (MIT Press, Cambridge, MA, 1987); L. N. Lipatov, in *Perturbative Quantum Chromodynamics*, edited by A. H. Mueller (World Scientific, Singapore, 1989), p. 411; V. Del Duca, Sci. Acta **10**, 91 (1995), hep-ph/9503226; L. N. Lipatov, Phys. Rep. **286**, 131 (1997).

 [5] A. H. Mueller, Eur. Phys. J. A **1**, 19 (1998); Phys. Lett. B **396**, 251 (1997).

 [6] W. Rühl, Kaiserslautern Report No. TP-2 1971; E. Wieczorek, V. A. Matveev, D. Robaschik, and A. N. Tavkhelidze, Teor. Mat. Fiz. **16**, 315 (1973) [Theor. Math. Phys. **16**, 861 (1973)]; B. I. Zavialov and S.I. Maksimov, Kiev Report No. ITF-75-77P, 1975; B. Geyer, D. Robaschik, and E. Wieczorek, Fortschr. Phys. **27**, 75 (1979).

 [7] R. Jost and H. Lehmann, Nuovo Cimento **5**, 1598 (1957); F. J. Dyson, Phys. Rev. **110**, 579 (1958).

 [8] S. Catani and F. Hautmann, Nucl. Phys. **B427**, 475 (1994).

 [9] G. Camici and M. Ciafaloni, Phys. Lett. B **386**, 341 (1996); Nucl. Phys. **B496**, 305 (1997).

[10] G. Camici and M. Ciafaloni, Phys. Lett. B **412**, 396 (1997).

[11] J. Blümlein, J. Phys. G **19**, 1623 (1993).

[12] J. Blümlein and A. Vogt, Phys. Rev. D **57**, 1 (1998).

[13] F. Bloch and A. Nordsieck, Phys. Rev. **52**, 54 (1937); D. R. Yennie, S. C. Frautschi, and H. Suura, Ann. Phys. (N.Y.) **13**, 379 (1961).

[14] T. Kinoshita, J. Math. Phys. **3**, 650 (1962); T. D. Lee and M. Nauenberg, Phys. Rev. **133**, B1549 (1964).

[15] D. J. Gross and F. Wilczek, Phys. Rev. Lett. **30**, 1343 (1973); H. D. Politzer, *ibid.* **30**, 1346 (1973).

[16] W. E. Caswell, Phys. Rev. Lett. **33**, 244 (1974); D. R. T. Jones, Nucl. Phys. **B75**, 531 (1974).

[17] O. V. Tarasov, A. A. Vladimirov, and A. Y. Zarkov, Phys. Lett. **93B**, 429 (1980); S. A. Larin and J. A. M. Vermaseren, Phys. Lett. B **303**, 334 (1993).

[18] T. van Ritbergen, J. A. M. Vermaseren, and S. A. Larin, Phys. Lett. B **400**, 379 (1997).

[19] A. D. Martin, R. G. Roberts, and W. J. Stirling, Phys. Lett. B **266**, 173 (1991); M. Virchaux and A. Milsztain, *ibid.* **274**, 221 (1992).

[20] J. Blümlein, S. Riemersma, W. L. van Neerven, and A. Vogt, in *QCD and QED in Higher Orders*, Proceedings of the Zeuthen Workshop, Rheinsberg, Germany, 1996, edited by J. Blümlein *et al.* [Nucl. Phys. B (Proc. Suppl.) **51C**, 97 (1996)].

[21] J. Blümlein and A. Vogt, Phys. Lett. B **370**, 149 (1996); Acta Phys. Pol. B **27**, 1309 (1996).

[22] R. Kirschner and L. N. Lipatov, Nucl. Phys. **B213**, 122 (1983).

[23] J. Blümlein, S. Riemersma, and A. Vogt, in *QCD and QED in Higher Orders* [20], p. 30.

[24] D. Gross and F. Wilczek, Phys. Rev. D **8**, 3633 (1973); **9**, 980 (1974); H. Georgi and D. Politzer, *ibid.* **9**, 416 (1974); L. N. Lipatov, Sov. J. Nucl. Phys. **20**, 94 (1975); G. Altarelli and G. Parisi, Nucl. Phys. **B126**, 298 (1977); K. Kim and K.

Schilcher, Phys. Rev. D **17**, 2800 (1978); Yu. Dokshitser, Sov. Phys. JETP **46**, 641 (1977).

[25] H. Ito, Prog. Theor. Phys. **54**, 555 (1975); K. Sasaki, *ibid.* **54**, 1816 (1975); M. Ahmed and G. Ross, Phys. Lett. **56B**, 385 (1975); Nucl. Phys. **B111**, 298 (1976); Altarelli and Parisi, [24].

[26] G. Floratos, D. Ross, and C. Sachrajda, Nucl. Phys. **B129**, 66 (1977); **B139**, 545(E) (1978); **B152**, 493 (1979); A. Gonzalez-Arroyo, C. Lopez, and F. Yndurain, *ibid.* **B153**, 161 (1979); A. Gonzalez-Arroyo and C. Lopez, *ibid.* **B166**, 429 (1980); G. Floratos, P. Lacaze, and C. Kounnas, Phys. Lett. **98B**, 89 (1981); Nucl. Phys. **B192**, 417 (1981); G. Curci, W. Furmanski, and R. Petronzio, *ibid.* **B175**, 27 (1980).

[27] G. Floratos, P. Lacaze, and C. Kounnas, Nucl. Phys. **B192**, 417 (1981); A. Gonzalez-Arroyo and C. Lopez, *ibid.* **B166**, 429 (1980); G. Floratos, P. Lacaze, and C. Kounnas, Phys. Lett. **98B**, 285 (1981); W. Furmanski and R. Petronzio, *ibid.* **97B**, 437 (1980); R. K. Ellis and W. Vogelsang, Report No. FERMILAB-PUB-96-044-T, hep-ph/9602356.

[28] R. Mertig and W. van Neerven, Z. Phys. C **70**, 637 (1996); W. Vogelsang, Phys. Rev. D **54**, 2023 (1996); Nucl. Phys. **B475**, 47 (1996).

[29] S. Larin, T. van Ritbergen, and J. Vermaseren, Nucl. Phys. **B427**, 41 (1994); S. Larin, P. Nogueira, T. van Ritbergen, and J. Vermaseren, *ibid.* **B492**, 338 (1997).

[30] R. J. De Witt *et al.*, Phys. Rev. D **19**, 2046 (1979); **20**, 1751(E) (1979).

[31] W. A. Bardeen and A. J. Buras, Phys. Rev. D **20**, 166 (1979); **21**, 2041(E) (1980); M. Fontannaz and E. Pilon, *ibid.* **45**, 382 (1992); **46**, 484(E) (1992).

[32] M. Glück, E. Reya, and A. Vogt, Phys. Rev. D **45**, 3986 (1992); **48**, 116 (1993).

[33] W. Furmanski and R. Petronzio, Z. Phys. C **11**, 293 (1982).

[34] M. Glück and E. Reya, Phys. Rev. D **25**, 1211 (1982).

[35] G. Altarelli, R. K. Ellis, and G. Martinelli, Nucl. Phys. **B157**, 461 (1979).

[36] For a summary of coefficient functions in the $\overline{\text{MS}}$ scheme to $O(\alpha_s)$ see Ref. [33] and references therein.

[37] E. Zijlstra and W. van Neerven, Nucl. Phys. **B383**, 525 (1992); Phys. Lett. B **297**, 377 (1993); Nucl. Phys. **B417**, 61 (1994); **B426**, 245(E) (1994); J. Sanchez Guillén *et al.*, *ibid.* **B353**, 337 (1991); S. Larin and J. Vermaseren, Z. Phys. C **57**, 93 (1993).

[38] E. Zijlstra and W. van Neerven, Phys. Lett. B **297**, 377 (1993); Nucl. Phys. **B417**, 61 (1994); **B426**, 245(E) (1994).

[39] A. Bassetto, M. Ciafaloni, and D. Marchesini, Phys. Rep. **100**, 201 (1983).

[40] D. Kreimer, J. Knot Theory Ramifications **6**, 479 (1997).

[41] S. Catani, F. Fiorani, and G. Marchesini, Nucl. Phys. **B336**, 18 (1990).

[42] R. D. Ball and S. Forte, Phys. Lett. B **351**, 313 (1995).

[43] J. Blümlein, in *QCD and High Energy Hadronic Interactions*, Proceedings of the XXXth Rencontres de Moriond, 1995, edited by J. Tran Thann Van (Edition Frontières, Paris, 1996), p. 191, hep-ph/9506446.

[44] R. K. Ellis, F. Hautmann, and B. Webber, Phys. Lett. B **348**, 582 (1995).

[45] M. Ciafaloni, Phys. Lett. B **356**, 74 (1995).

[46] S. Catani, M. Ciafaloni, and F. Hautmann, Nucl. Phys. **B366**, 135 (1991).

[47] V. S. Fadin and L. N. Lipatov, Yad. Fiz. **50**, 1141 (1989) [Sov. J. Nucl. Phys. **50**, 712 (1989)]; Nucl. Phys. **B406**, 259 (1993); **B477**, 767 (1996); V. S. Fadin, M. I. Kotskii, and L. N. Lipatov, Report No. BUDKERINP-97-56; V. S. Fadin, R. Fiore, and A. Quartalo, Phys. Rev. D **50**, 2265 (1994); **50**, 5893 (1994); V. S. Fadin, R. Fiore, and M. I. Kotskii, Phys. Lett. B **359**, 181 (1995); **387**, 593 (1996); V. S. Fadin, R. Fiore, A. Fladi, and M. I. Kotskii, *ibid.* **422**, 287 (1998).

[48] V. Del Duca, Phys. Rev. D **54**, 989 (1996); **54**, 4474 (1996); V. Del Duca and C. R. Schmidt, *ibid.* **57**, 4069 (1998).

[49] C. Coriano and A. R. White, Nucl. Phys. **B468**, 175 (1996); C. Coriano, R. R. Parwani, and A. R. White, *ibid.* **B468**, 217 (1996); C. Coriano, A. R. White, and M. Wüsthoff, *ibid.* **B493**, 397 (1997).

[50] B.W. Char *et al.*, MAPLE-V Reference Manual (Springer, Berlin, 1991).

[51] R. D. Ball and S. Forte, Phys. Lett. B **358**, 365 (1995).

[52] J. Forshaw, R. Roberts, and R. Thorne, Phys. Lett. B **356**, 79 (1995).

[53] R. Thorne, Phys. Lett. B **392**, 463 (1997); Nucl. Phys. **B512**, 323 (1998); I. Bojak and M. Ernst, Phys. Lett. B **397**, 296 (1997); Nucl. Phys. **B508**, 731 (1997).

[54] B. M. McCoy and T. T. Wu, Phys. Lett. **71B**, 97 (1977).

[55] J. Blümlein and A. Vogt, Phys. Lett. B **386**, 350 (1996).

[56] For a uniqueness theorem, see E. Carlson, Ph.D. thesis, University of Uppsala, 1914; E. C. Titchmarsh, *Theory of Functions* (Oxford University Press, Oxford, 1939), Chap. 9.5.

[57] M. Glück, E. Reya, and A. Vogt, Z. Phys. C **48**, 471 (1990).

[58] C. Berger, D. Graudenz, M. Hampel, and A. Vogt, Z. Phys. C **70**, 77 (1996).

[59] R. K. Ellis, E. Levin, and Z. Kunszt, Nucl. Phys. **B420**, 517 (1994); **B433**, 498(E) (1995).

[60] For older approaches see Refs. [46,48] in J. Blümlein, Surv. High Energy Phys. **7**, 161 (1994); M. Virchaux and A. Oraou, Report No. DphPE 87-15; M. Virchaux, Ph.D. thesis, Université Paris-7, 1988; A. Oraou, Ph.D. thesis, Université Paris-11, 1988; M. Botje, ''QCDNUM15: A fast QCD evolution program''; C. Pascaud and F. Zomer, H1 Note: H1-11/94-404.

[61] CTEQ Collaboration, H. L. Lai *et al.*, Phys. Rev. D **55**, 1280 (1997).

[62] A. D. Martin, R. G. Roberts, and W. J. Stirling, Phys. Lett. B **354**, 155 (1995).

[63] M. Diemoz, F. Ferroni, E. Longo, and G. Martinelli, Z. Phys. C **39**, 21 (1988).

[64] M. Glück, E. Reya, and A. Vogt, Z. Phys. C **53**, 127 (1992); **67**, 433 (1995).

[65] A. De Rujula, S. L. Glashow, H. D. Politzer, S. B. Treiman, F. Wilczek, and A. Zee, Phys. Rev. D **10**, 1649 (1974); T. De Grand, Nucl. Phys. **B151**, 485 (1979); J. P. Ralston and D.W. McKay, in *Physics Simulations at High Energies*, edited by V. Barger (World Scientific, Singapore, 1987), p. 30; J. Blümlein, Surv. High Energy Phys. **7**, 161 (1994).

[66] Cf., e.g., R. D. Ball and S. Forte, Phys. Lett. B **336**, 77 (1994).

[67] E. Laenen, S. Riemersma, J. Smith, and W. van Neerven, Phys. Lett. B **291**, 325 (1992); Nucl. Phys. **B392**, 162 (1993); **B392**, 229 (1993); M. Glück, E. Reya, and M. Stratmann, *ibid.* **B422**, 37 (1994); S. Riemersma, J. Smith, and W. van Neerven, Phys. Lett. B **347**, 143 (1995); A. Vogt, in *Proceedings of the 4th International Conference on Deep Inelastic Scattering and Related Phenomena*, Rome, 1996, edited by G. D'Agostini and A. Nigro (World Scientific, Singapore, 1997), p. 254, hep-ph/9601352; J. Blümlein and S. Riemersma, in *Future Physics at HERA*, Proceedings of the Workshop 1995/96, edited by G. Ingelman *et al.* (DESY, Hamburg, 1996), Vol. 1, p. 82, hep-ph/9609394; E. Laenen *et al.*, *ibid.*, p. 393, hep-ph/9609351; M. Buza, Y. Matiounine, J. Smith, and W. van Neerven, Nucl. Phys. **B472**, 611 (1996); Phys. Lett. B **411**, 211 (1997); Nucl. Phys. **B485**, 420 (1997); Eur. Phys. J. C **1**, 301 (1998); M. Aivazis, F. Olness, and Wu-Ki Tung, Phys. Rev. D **50**, 3085 (1994); M. Aivazis, J. C. Collins, F. Olness, and Wu-Ki Tung, *ibid.* **50**, 3102 (1994); Wu-Ki Tung, in *Deep Inelastic Scattering and Related Phenomena*, Chicago, 1997, edited by J. Repond and D. Krakauer, AIP Conf. Proc. 407 (American Institute of Physics, New York, 1997), p. 1014, and references therein; C.R. Schmidt, *ibid.*, p. 381; J. C. Collins, A. D. Martin, and M. G. Ryskin, in *Proceedings of the International Conference on Low x Physics at HERA*, Miraflores, Spain, 1997, edited by F. Barreiro (World Scientific, Singapore, 1998), hep-ph/9709440; R. S. Thorne and R. G. Roberts, Phys. Rev. D **57**, 6871 (1998); Phys. Lett. B **421**, 303 (1998).

[68] J. Blümlein, M. Botje, C. Pascaud, S. Riemersma, W. L. van Neerven, A. Vogt, and F. Zomer, in *Future Physics at HERA* [67], Vol. 1, p. 23, hep-ph/9609400.

[69] A. Zee, F. Wilczek, and S. B. Treiman, Phys. Rev. D **10**, 2881 (1974).

[70] M. Glück, E. Reya, and A. Vogt, Phys. Rev. D **46**, 1973 (1992).

[71] P. Aurenche, J. P. Guillet, and M. Fontannaz, Z. Phys. C **64**, 621 (1994); G. Schuler and T. Sjostrand, *ibid.* **68**, 607 (1995).

[72] A. Vogt, in *Proceedings of the Conference Structure and Interactions of the Photon, PHOTON'97*, Egmond aan Zee, The Netherlands, edited by A. Buijs and F. C. Erné (World Scientific, Singapore, 1998), p. 3, hep-ph/9709345.

[73] D. J. Miller and A. Vogt, in *Proceedings of the Workshop $e^+e^-$ Collisions at TeV Energies: The Physics Potential*, edited by P. M. Zerwas (DESY Report No. 96-123D, Hamburg, Germany, 1996), p. 473.

[74] J. Bartels, A. DeRoeck, and H. Lotter, Phys. Lett. B **389**, 742 (1996); S. J. Brodsky, F. Hautmann, and D. Soper, Phys. Rev. Lett. **78**, 803 (1997); **79**, 3544(E) (1997); Phys. Rev. D **56**, 6957 (1997).

[75] J. Blumlein, V. Ravindran, W. van Neerven, and A. Vogt, in the Proceedings of the 6th International Workshop on Deep Inelastic Scattering and QCD, Brussels, 1998.